



Sandia  
National  
Laboratories

# Density effects on plasma spectroscopy

Stephanie Hansen  
*Sandia National Labs*



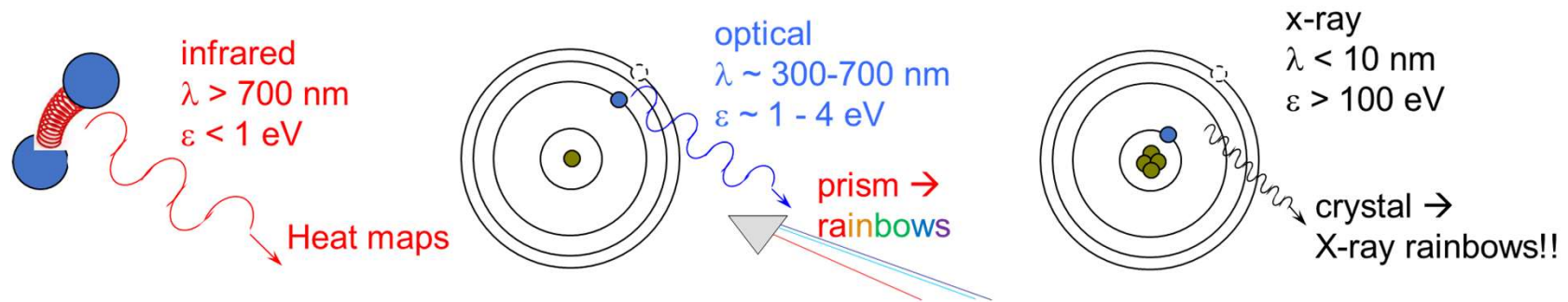
2023 Atomic Processes in Plasmas



Sandia National Laboratories is a multimission laboratory managed and operated by National Technology & Engineering Solutions of Sandia, LLC, a wholly owned subsidiary of Honeywell International Inc., for the U.S. Department of Energy's National Nuclear Security Administration under contract DE-NA0003525.

**SAND2023-02978PE**

# Spectroscopy tells us about the basic structure of matter

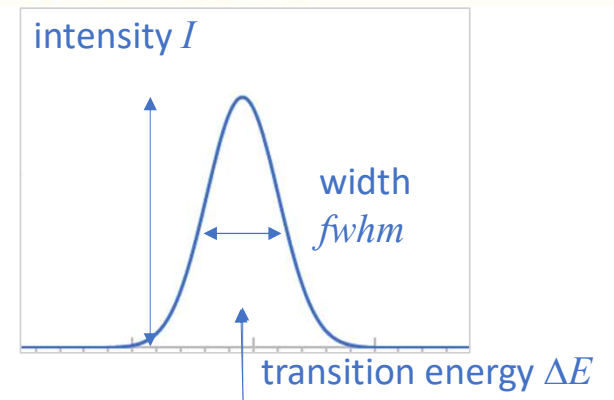
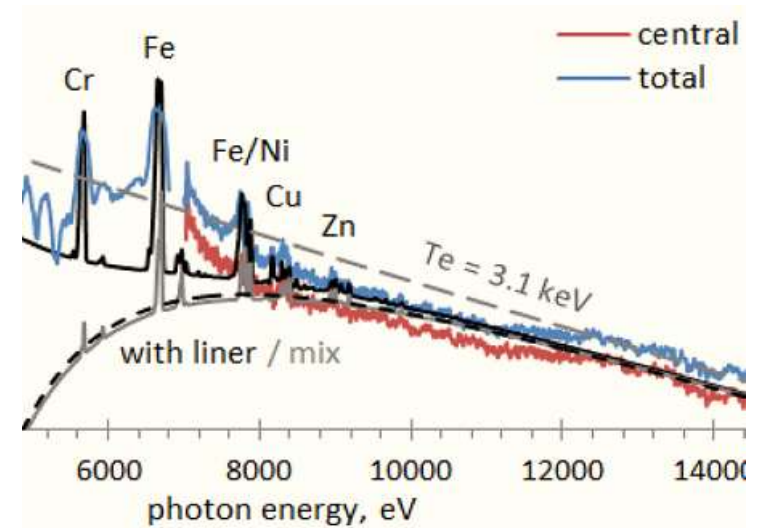
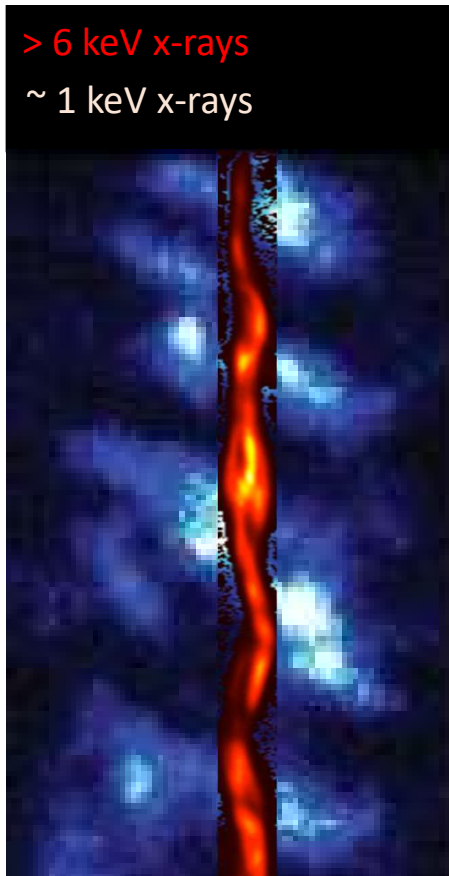


Probing material at different wavelengths/ energies allows us to probe different physical phenomena, from thermal motion to electronic structure

For highly ionized plasmas, low-energy emission is often dominated by collective effects and/or optically thick, so X-rays are particularly useful

# For many HED plasmas, a spectrum is worth a thousand pictures

- Coarse energy resolution in imaging can reveal plasma gradients
- Fine energy resolution (spectroscopy) can reveal details of plasma composition, temperature, and density
- Each emission or absorption line is characterized by its wavelength (energy), intensity, and width (or shape)
- Interpreting spectra requires understanding atomic-scale structure and response



# There are two categories of density effects we can see with spectroscopy

---

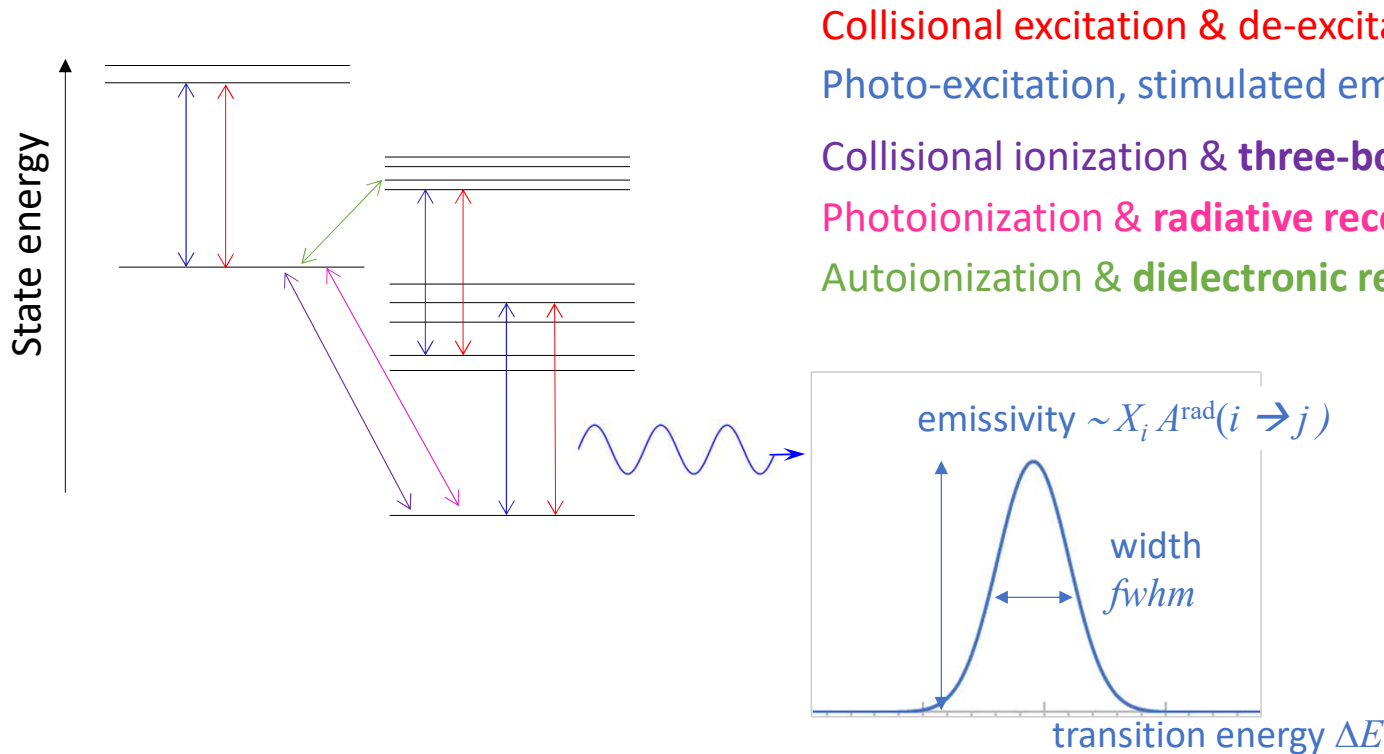
1. Atomic kinetic effects – Collisional radiative models
  - a. Ladder ionization
  - b. Metastable states
  - c. Degenerate electron distributions
  
2. Atomic structure effects – Density functional theory models
  - a. Plasma screening
  - b. Pressure ionization
  - c. Line broadening



# Collisional-radiative models are foundational to x-ray spectroscopy

Collisional-radiative models (Ralchenko) are built from states (Gu) and rates (Fontes, Ballance, Gu)

Collisional-radiative models balance rates into and out of each state:  $dX_i/dt = \sum_j X_j R_{ji} - X_i \sum_j R_{ij}$



Collisional excitation & de-excitation

Photo-excitation, stimulated emission, & radiative decay

Collisional ionization & **three-body recombination**

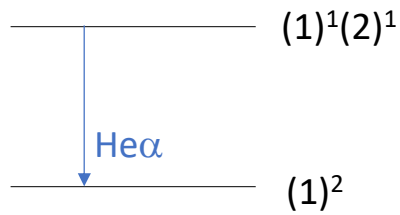
Photoionization & **radiative recombination**

Autoionization & **dielectronic recombination**

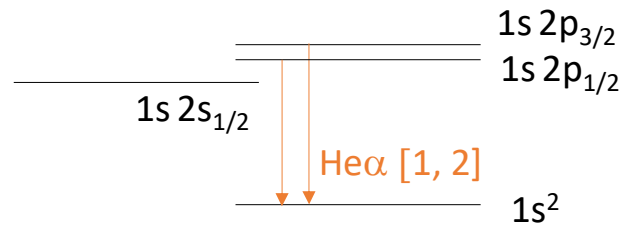
If you know state populations  $X_i$ , radiative decay rates  $A^{\text{rad}}$ , and line profiles, you can compute a spectrum!

# Electronic states can be treated with varying levels of detail

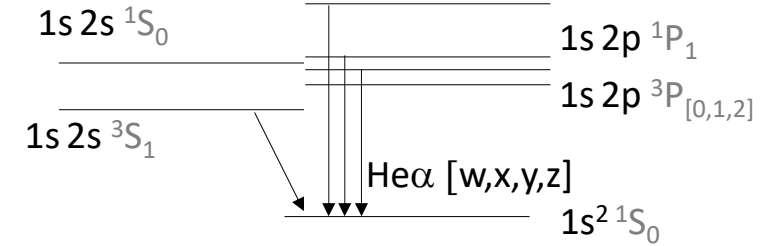
## Superconfigurations



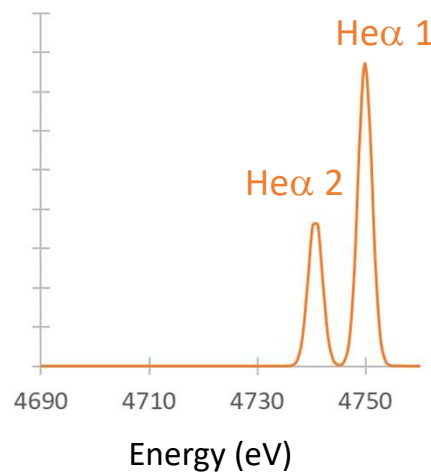
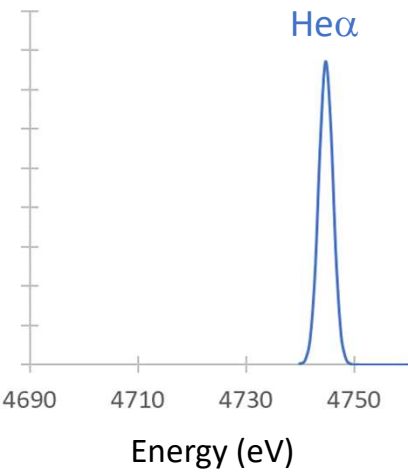
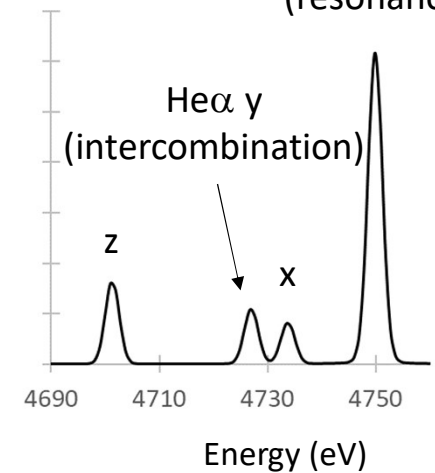
## Configurations



## Detailed structure

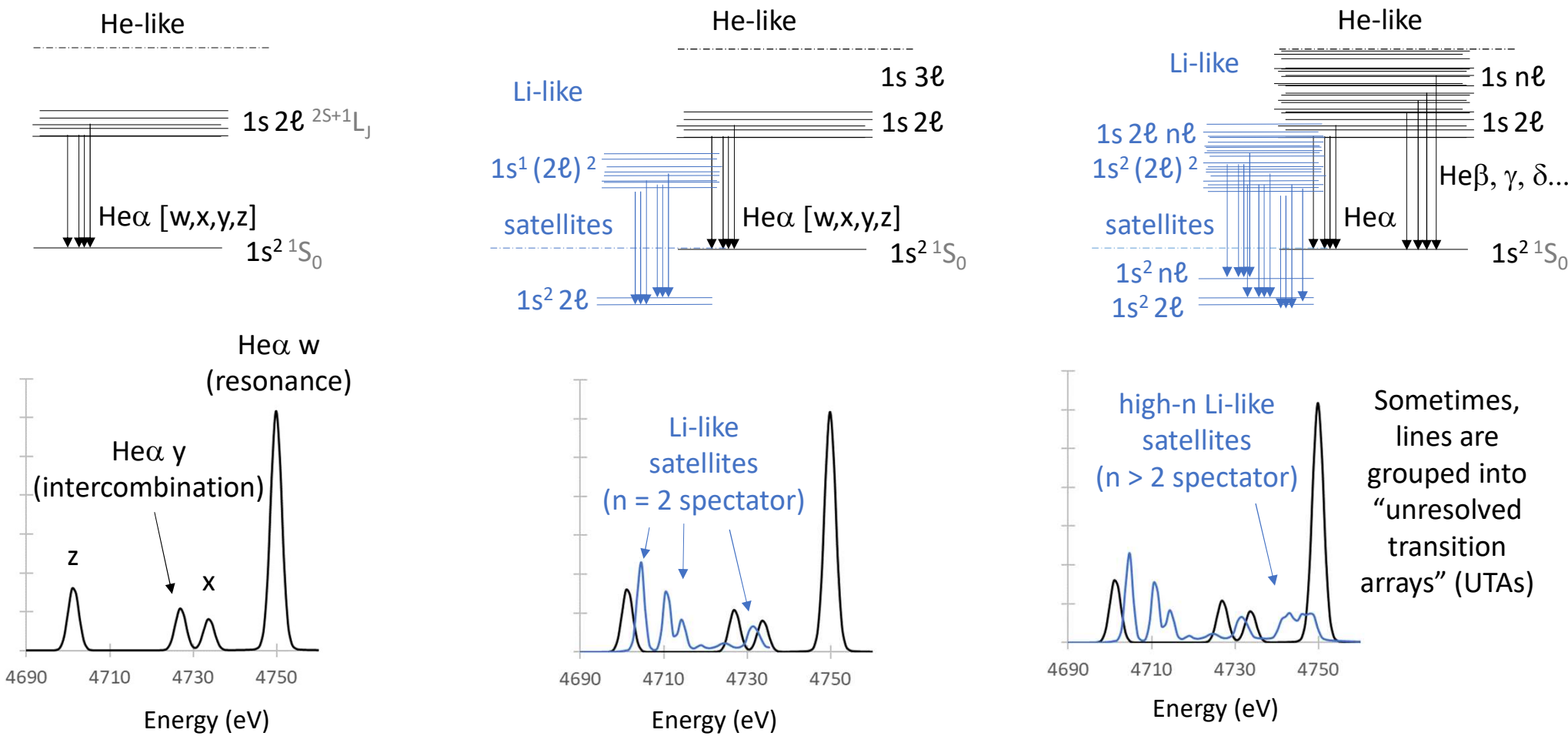


## Heα w (resonance)



Generally, we need fairly detailed state structure to reliably diagnose experiments

# Different degrees of completeness also modify modeled spectra

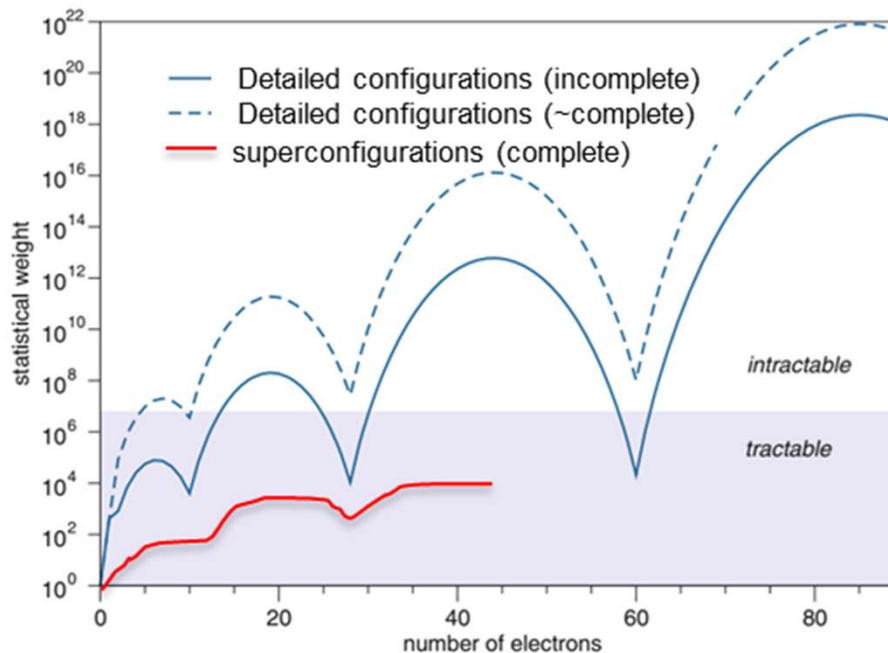


# Unfortunately, complete & detailed CR models can become intractable

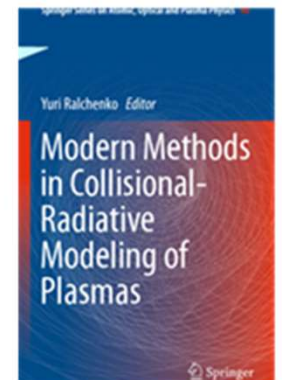
The combinatorics of detailed electronic structure can be daunting: the most detailed models (and real ions) have  $N \sim \sum_i g_i$

CR models must calculate all rates among all states and invert the rate matrix to find the occupations  $X_i$  needed to compute line intensities

Thus, many CR models use less detailed states (configurations or superconfigurations) – or hybrid structure representations



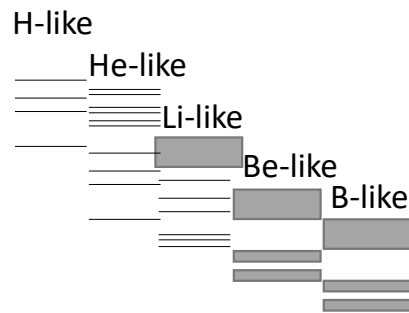
2016  
Ed. Yu. Ralchenko



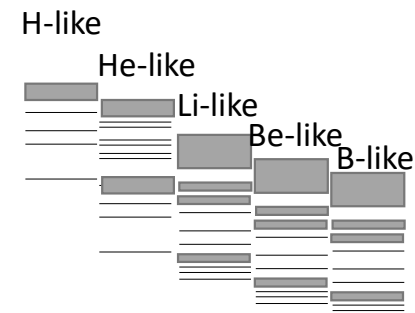


# Different CR models take different approaches to state structure

No CR model can be fully detailed, statistically complete, AND computationally tractable.  
Different modelers make different choices to balance detail, completeness, and speed

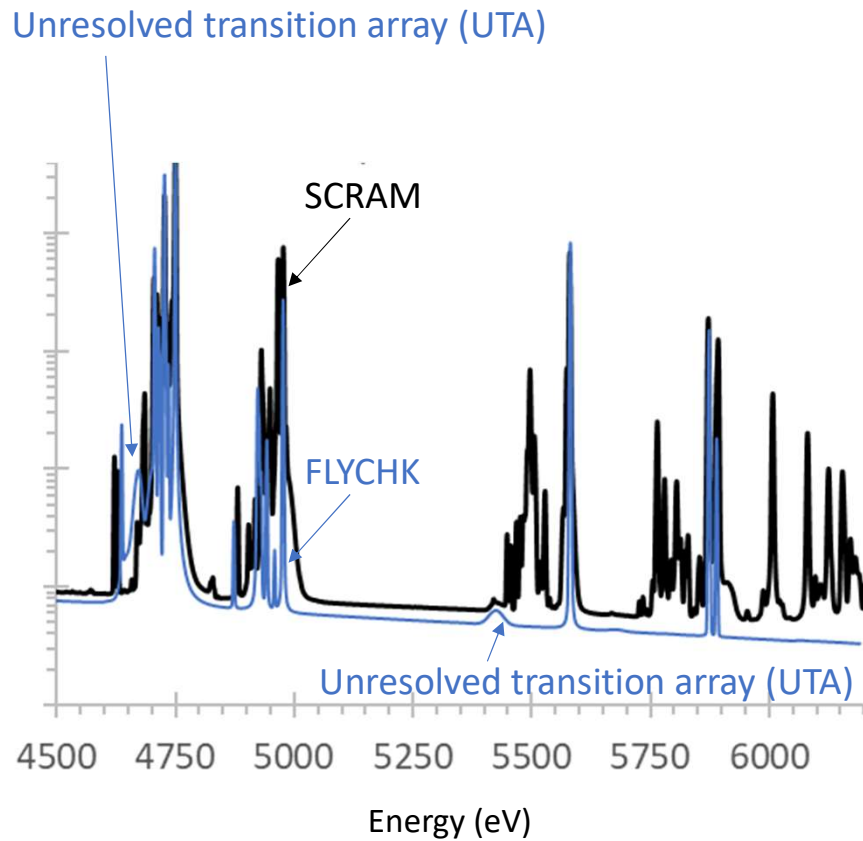


FLYCHK uses mostly  
superconfigurations, limiting  
detail to some K-shell ions  
→ runs in seconds



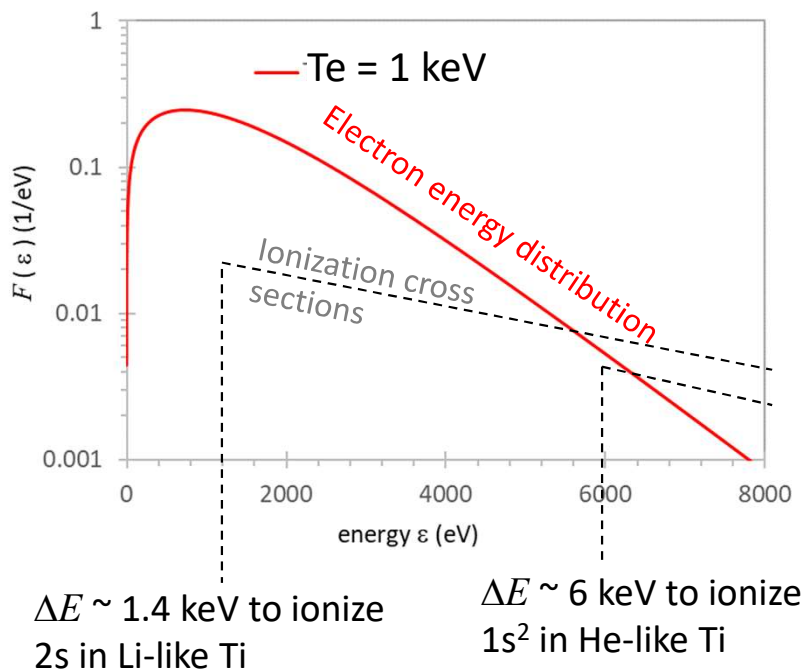
SCRAM mixes detailed states with  
configurations & superconfigurations,  
retaining some detail for every ion  
→ runs in minutes

# Differences in modeled structure are reflected in modeled spectra



No model is perfect:  
understanding model limitations &  
uncertainties is a critical part of  
spectroscopic diagnostics

# Rates are an additional source of model differences



Collisional rates are calculated by integrating cross sections over the electron energy distribution  $F(\varepsilon)$

Cross sections can be calculated in a wide variety of ways (see Fontes, Ballance, Gu)

In classical (non-degenerate) plasmas, the electron energy distribution is Maxwellian:

$$F_M(\varepsilon) = 2/T_e^{3/2} (\varepsilon/\pi)^{1/2} e^{-\varepsilon/T_e}$$

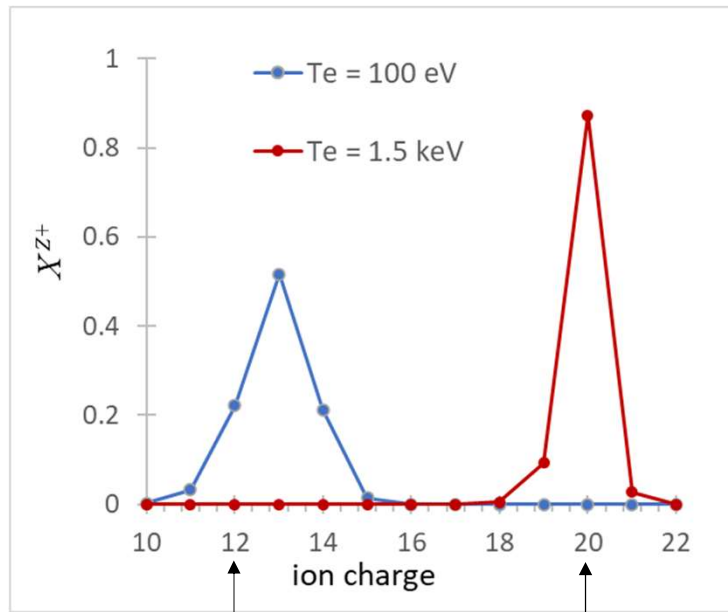
While downward rates sample all of the electrons, upward rates can only happen when impact electron energies are above some threshold (e.g. the ionization potential)

# State and ion populations are thus strongly dependent on temperature

We can sum up the state occupation probabilities  $X_i$  in different ways:

Charge state distributions (CSDs)

$$X^{Z+} = \sum_i X_i \text{ for all } i \text{ in ion with charge } Z+$$



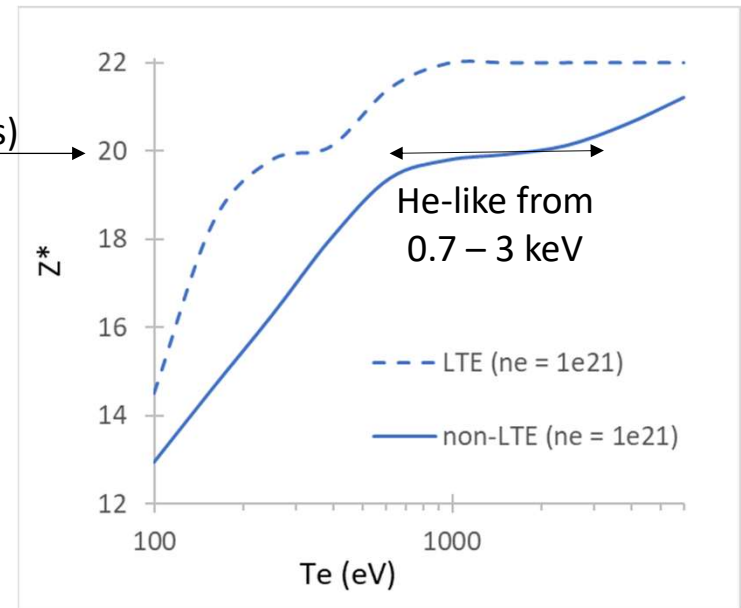
Ne-like Ti  
(10 electrons)

He-like Ti  
(2 electrons)

Average ionization  $Z^*$  ( $Z_{\text{bar}}$ ,  $\langle Z \rangle$ )

$$Z^* = \sum (Z+) X^{Z+}$$

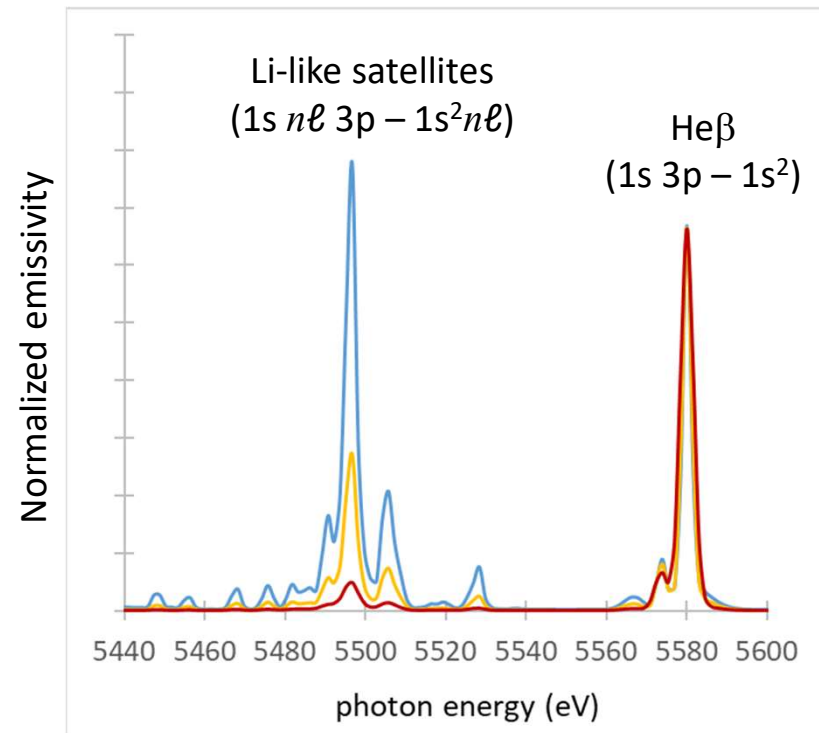
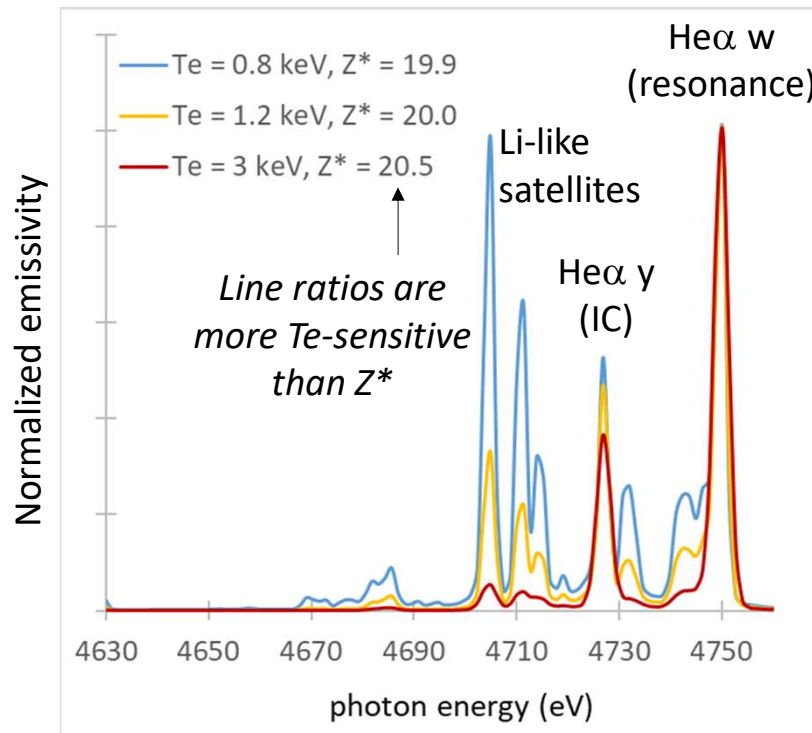
He-like Ti  
(2 electrons)  
closed shell



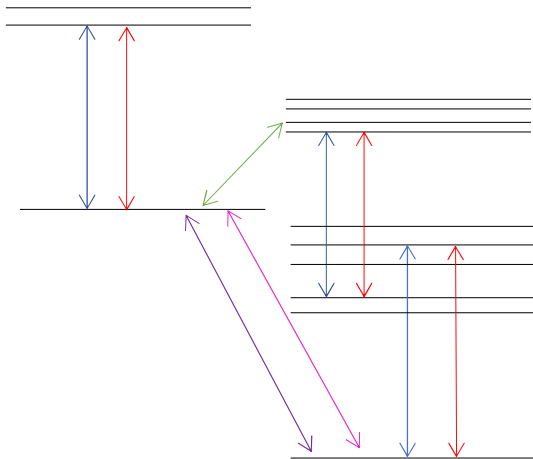
The average ion charge is most sensitive to temperature away from closed shells

# This temperature sensitivity is also reflected in emission spectra

For a given electron density, ratios of Li-like satellites to He $\alpha$  and He $\beta$  lines are good “thermometers”



# Rates also depend on the electron density



Collisional excitation & de-excitation  $\sim n_e^1$

Photo-excitation, stimulated emission, & radiative decay  $\sim n_e^0$

Collisional ionization  $\sim n_e^1$  & **three-body recombination**  $\sim n_e^2$

Photoionization  $\sim n_e^0$  & **radiative recombination**  $\sim n_e^1$

Autoionization  $\sim n_e^0$  & **dielectronic recombination**  $\sim n_e^1$

$R^{ion}/R^{rec} \sim (1/n_e) \exp(-\Delta E/T_e)$  for all ionization rate pairs.

For  $T_r = 0$ ,

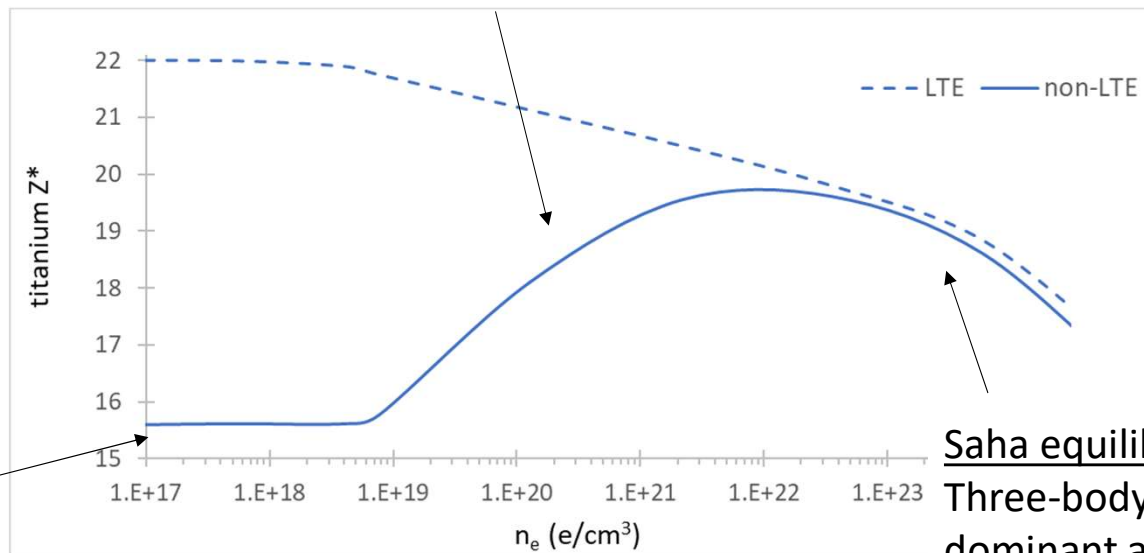
At low densities, collisional ionization ( $\sim n_e^1$ ) balances with radiative & dielectronic recombination ( $\sim n_e^1$ ):  $X^{Z+1}/X^Z \sim \exp(-\Delta E/T_e) \rightarrow$  coronal

At high densities, collisional ionization ( $\sim n_e^1$ ) balances with three-body recombination ( $\sim n_e^2$ ):  $X^{Z+1}/X^Z \sim (1/n_e) \exp(-\Delta E/T_e) \rightarrow$  Saha/LTE

# Balancing rates leads to complex density dependence in $Z^*$

## Ladder ionization

Excitation-ionization processes boost ionization;  
lead to increasing  $Z^*$  with  $n_e$



## Coronal equilibrium

Balance of collisional ionization with radiative & dielectronic recombination is independent of  $n_e$

## Saha equilibrium

Three-body recombination becomes dominant and enforces detailed balance with collisional ionization;  
 $Z^*$  decreases with  $n_e$

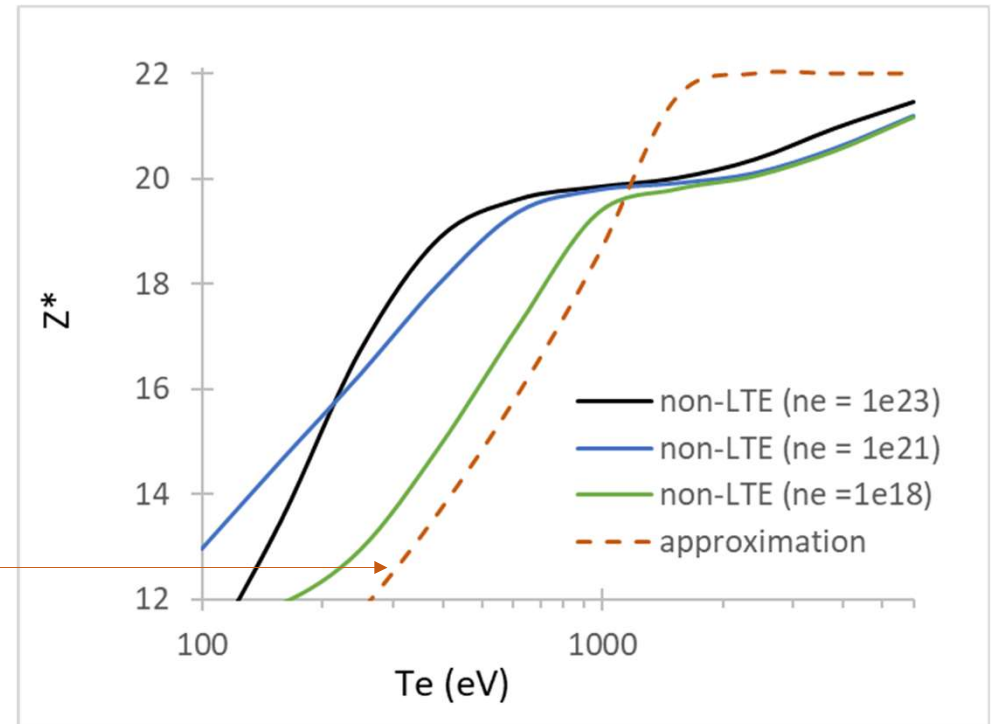
# $Z^*$ thus depends on both temperature and density

If you have at least a rough idea of density, obtaining  $Z^*$  from spectroscopy is a good thermometer. Otherwise, use caution.

In the low density/ coronal regime (e.g. tokamak, EBIT, solar corona),  $Z^*$  can give a first estimate of temperature by inverting the simple (*very rough!!*) approximation:

$$Z^* \sim (2/3) [Z_{nuc} T_e (\text{eV})]^{1/3}$$

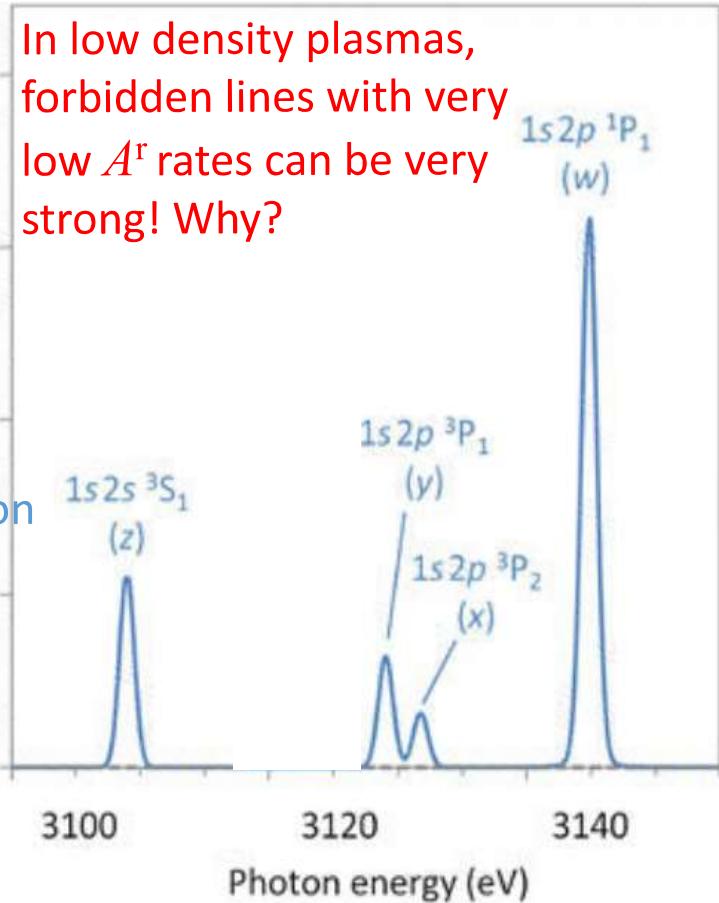
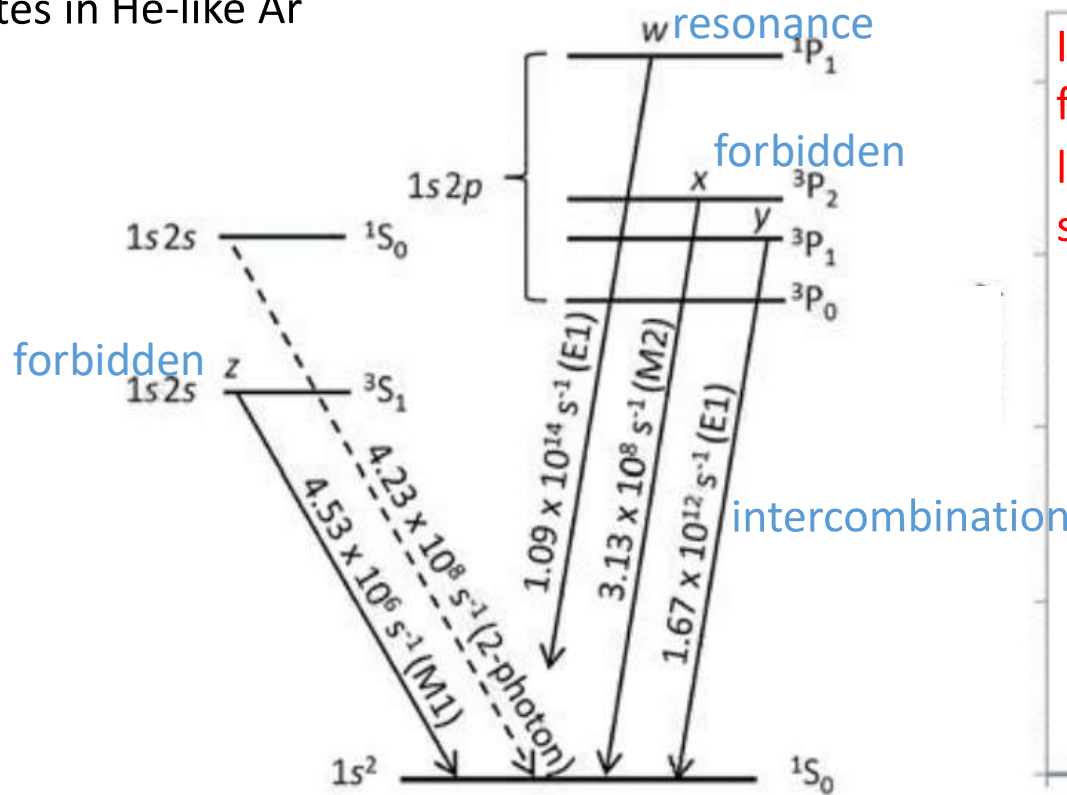
But it's better to directly diagnose density and use a trusted CR model





# Sometimes, we can use line ratios to estimate density

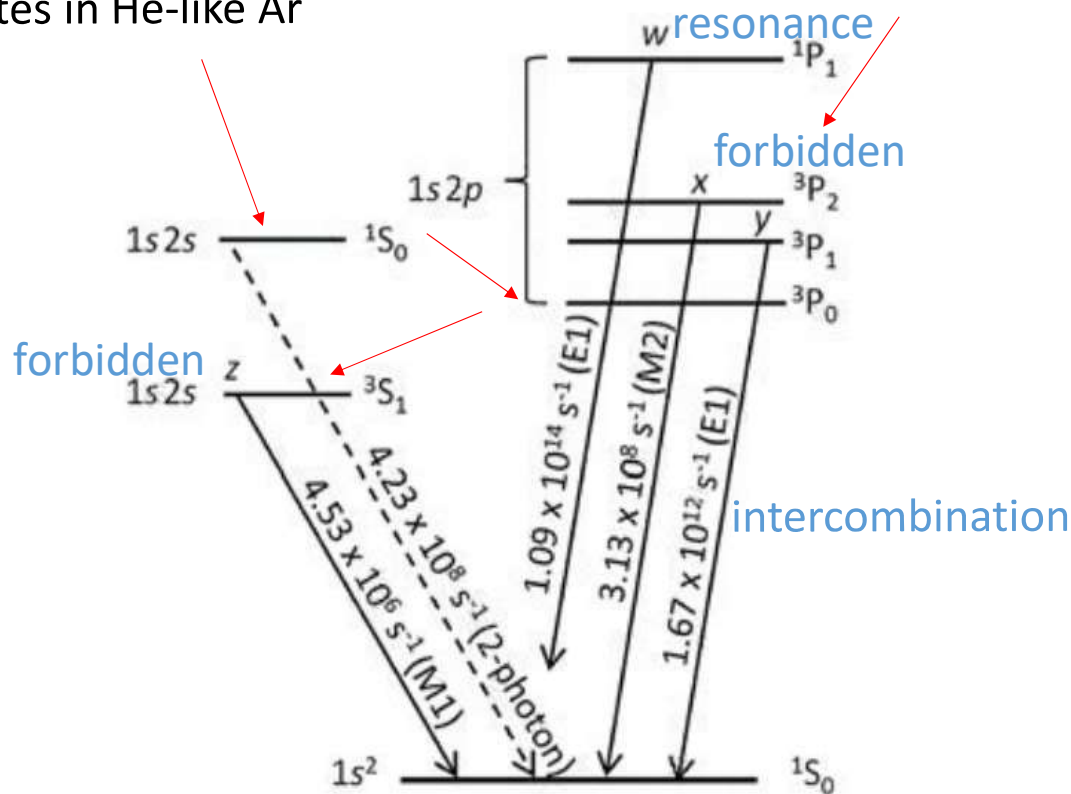
States in He-like Ar



In low density plasmas, forbidden lines with very low  $A^r$  rates can be very strong! Why?

# Sometimes, we can use line ratios to estimate density

States in He-like Ar

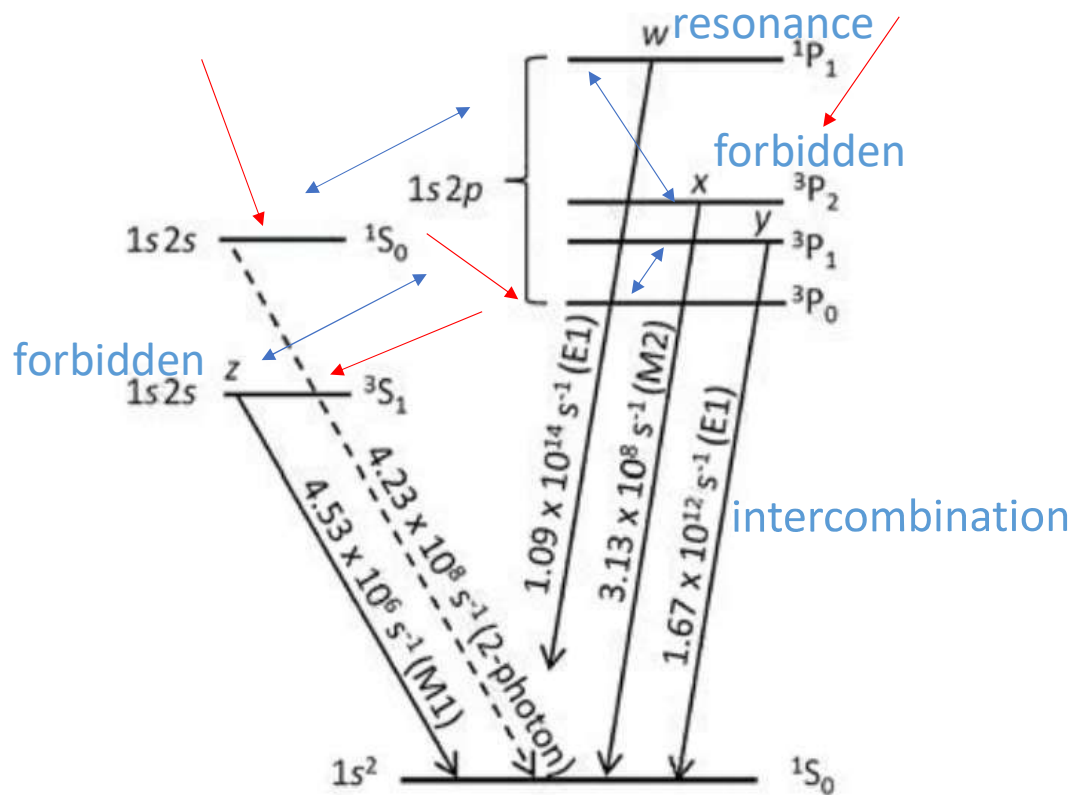


Recall that emissivity  $\eta_{i0} = X_i A_{i0}^r$

The only way we can get a strong signal from a “forbidden” transition with a very small  $A_{i0}^r$  is to have a very large  $X_i$

In the low density/coronal limit, low-lying “metastable” states with small  $A_{i0}^r$  can collect a significant fraction of the total population from **radiative cascades**

# Sometimes, we can use line ratios to estimate density



Recall that emissivity  $\eta_{i0} = X_i A_{i0}^r$

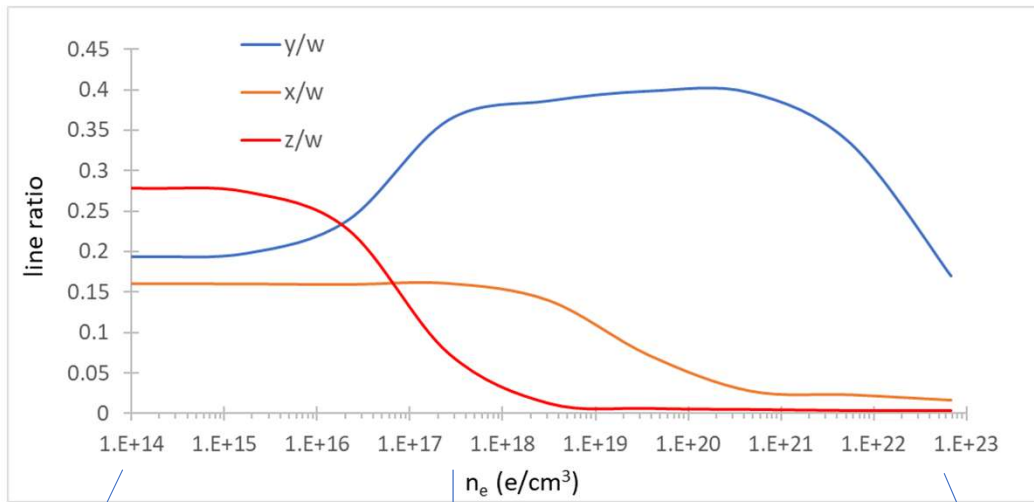
The only way we can get a strong signal from a “forbidden” transition with a very small  $A_{i0}^r$  is to have a very large  $X_i$

In the low density/coronal limit, low-lying “metastable” states with small  $A_{i0}^r$  can collect a significant fraction of the total population from radiative cascades

As density increases, **collisional excitation and de-excitation** move populations towards their LTE limit:

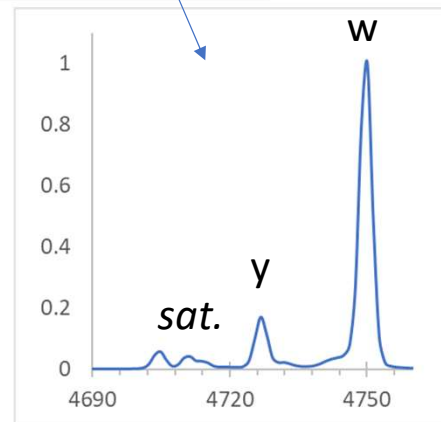
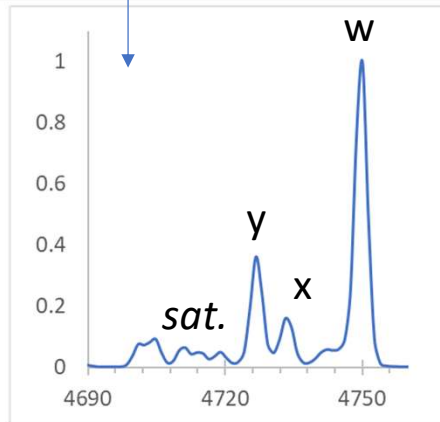
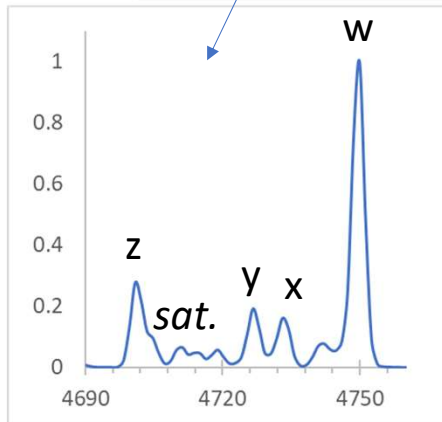
$$X_i = (g_i / g_0) \exp(-\Delta E_{i0} / T_e)$$

# Line ratios within ions are sensitive to the electron density



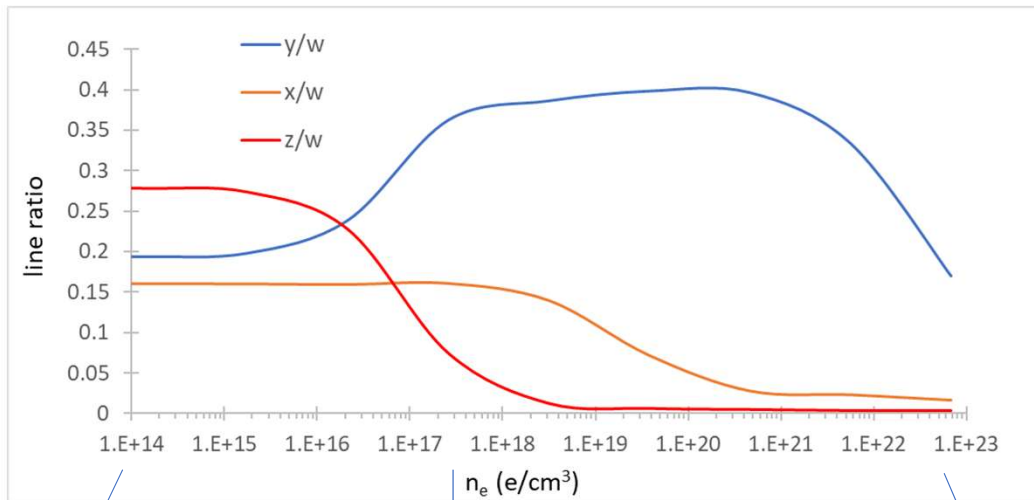
As density modifies the balance of collisional and radiative rates, state populations are redistributed and relative line intensities change significantly.

Intensity ratios within satellite complexes also change, but the most pronounced dependence is in closed-shell ions (He-like, Ne-like, Ni-like)



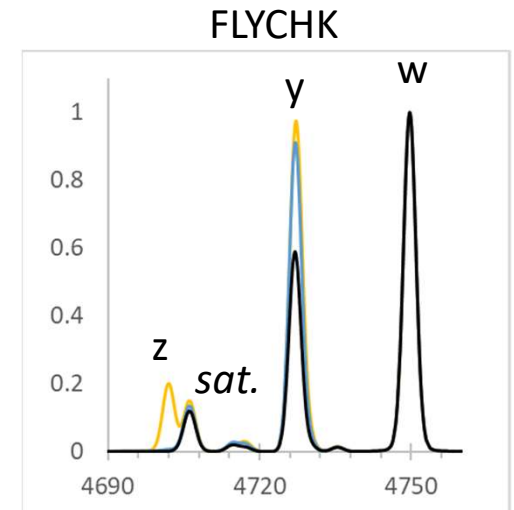
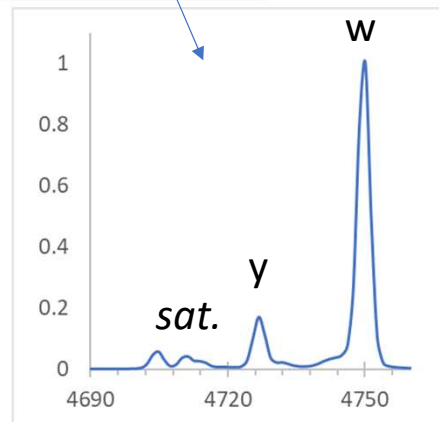
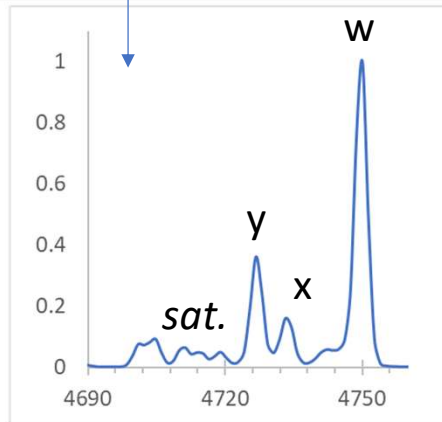
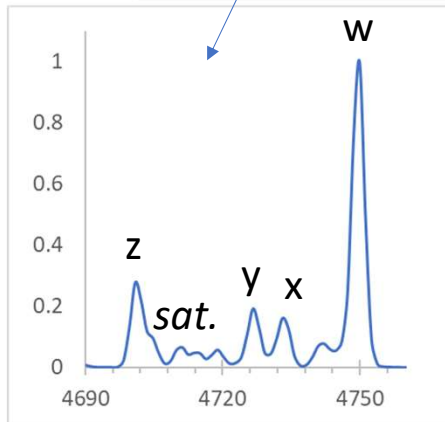
# Density-dependent line ratios can be highly model dependent

SCRAM



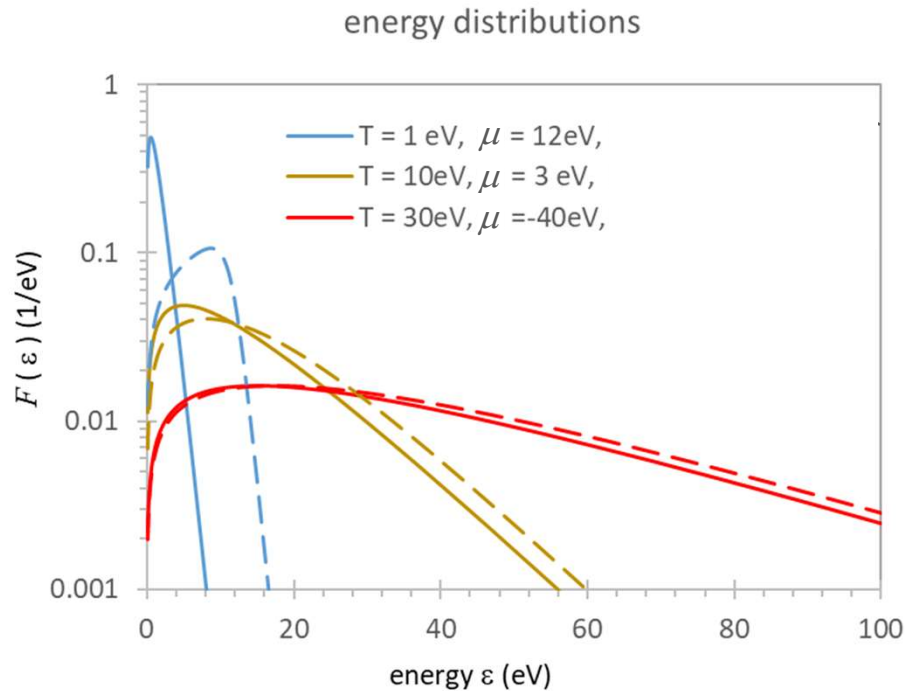
Why?

- Cascades depend on model completeness
  - Accurate balancing of collisional and radiative rates requires detailed states and high-order transitions
- Use these ratios with care!



Stephanie Hansen (sbhans@sandia.gov)

# At high density, degeneracy modifies free-electron distributions



Example: aluminum at  $2.7 \text{ g/cm}^3$  ( $n_i = 6 \times 10^{22} \text{ cm}^{-3}$ )

In classical plasmas, the electron energy distribution is Maxwellian:

$$F_M(\varepsilon) = 2/T_e^{3/2} (\varepsilon/\pi)^{1/2} e^{-\varepsilon/T_e}$$

At low  $T_e$  and high  $n_e$ , even free electrons are forced into close proximity. Since identical fermions cannot occupy identical states, the distribution function becomes:

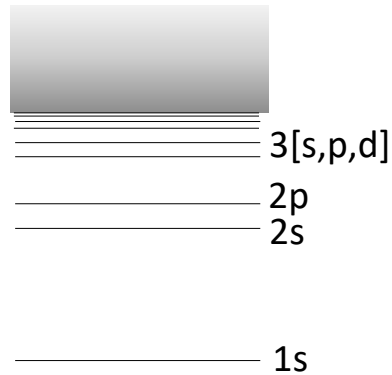
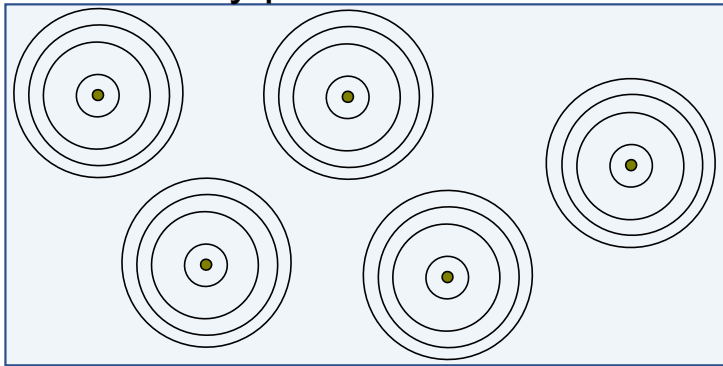
$$F_{\text{FD}}(\varepsilon) = (2\varepsilon)^{1/2} / (n_i Z^* \pi^2) [1 + e^{(\varepsilon - \mu)/T_e}]^{-1}$$

Note that we have introduced a new state variable,  $\mu$ , which is directly related to the electron density.

**These changes (and associated Pauli blocking) affect collisional rates – but not all CR models account for degeneracy effects**

# Very high plasma densities modify electronic structure

low-density plasma



In low-density plasmas, ions are isolated from each other and interact with a uniform background of ideal (uniform) free electrons

A puzzle:

statistical weights  $g_n = 2n^2 \rightarrow \infty$  for high  $n$

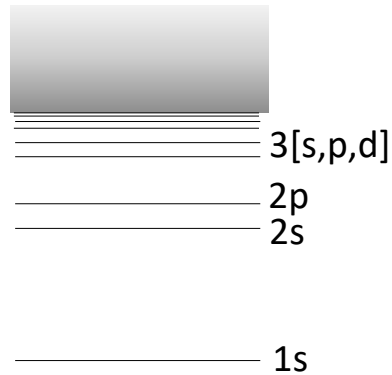
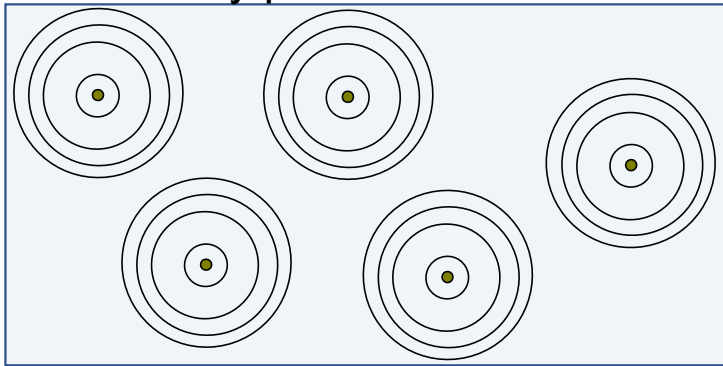
binding energies  $\varepsilon_n = -13.6 \text{ eV } (Z_{\text{eff}}/n)^2 \rightarrow 0$  for high  $n$

then occupations  $X_n = g_n \exp(-\varepsilon_n/T_e) \rightarrow \infty$  for high  $n$

.... But infinities are always problematic

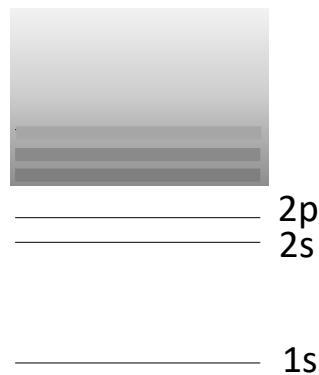
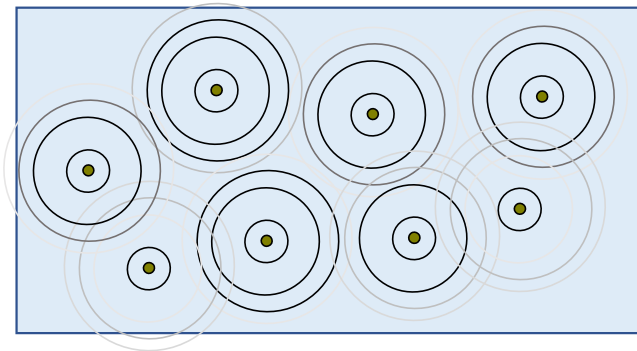
# Very high plasma densities modify electronic structure

low-density plasma



In low-density plasmas, ions are isolated from each other and interact with a uniform background of ideal (uniform) free electrons

high-density plasma

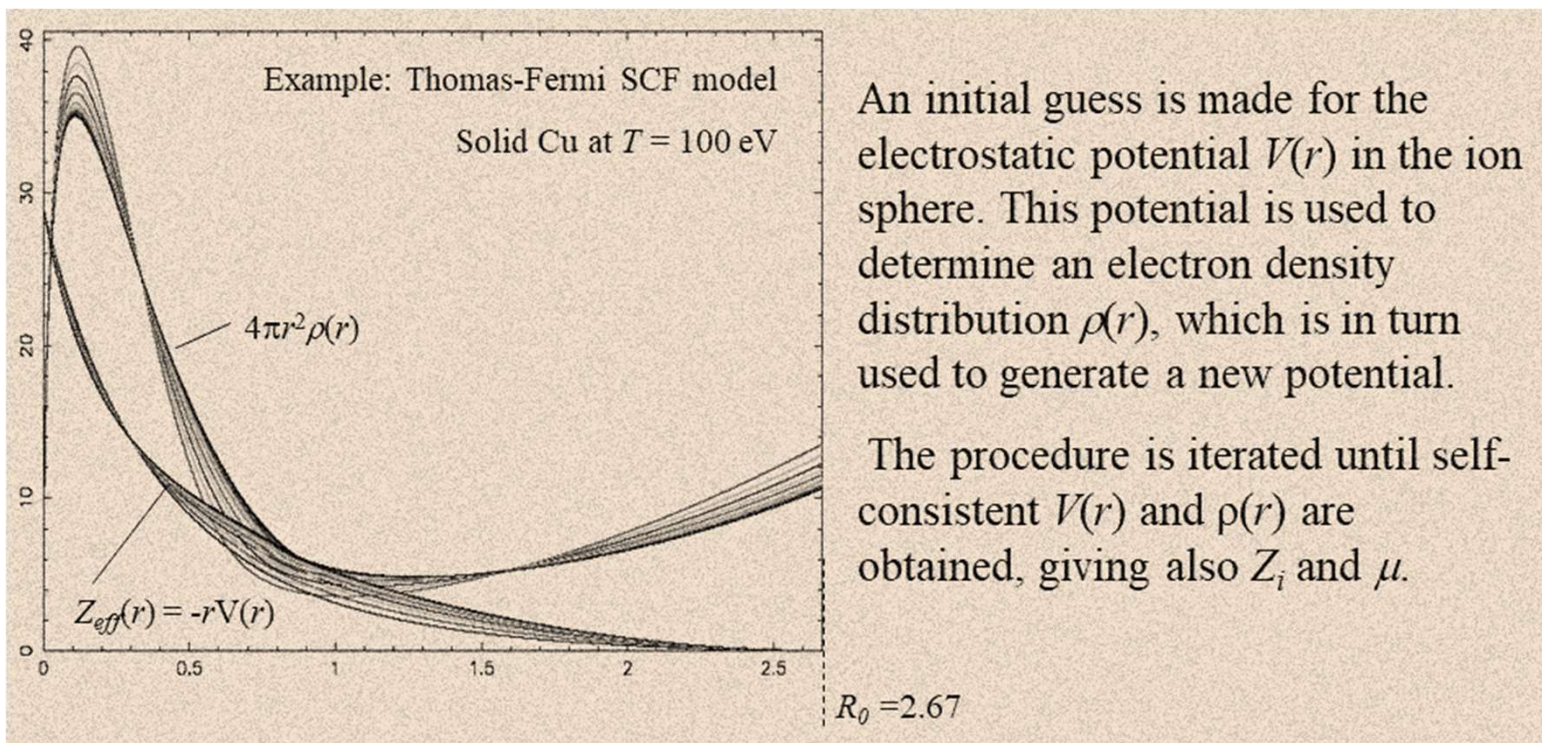


In high-density plasmas, neighboring ions perturb each other and respond to increasing screening from background free electrons: bound states “dissolve” into the continuum (related to band structure in solids) and their effective statistical weight decays (no infinities!)



# A brief excursion into density functional theory

Self-consistent-field (SCF) Thomas-Fermi models developed in the 1920s treat electrons as a degenerate fluid that screens the nuclear charge, giving  $\mu$ ,  $Z^*$ , pressure & energy



An initial guess is made for the electrostatic potential  $V(r)$  in the ion sphere. This potential is used to determine an electron density distribution  $\rho(r)$ , which is in turn used to generate a new potential.

The procedure is iterated until self-consistent  $V(r)$  and  $\rho(r)$  are obtained, giving also  $Z_i$  and  $\mu$ .

$$\rho \sim \int \frac{\sqrt{\epsilon}}{1 + e^{(\epsilon + V - \mu)/\tau}} d\epsilon$$

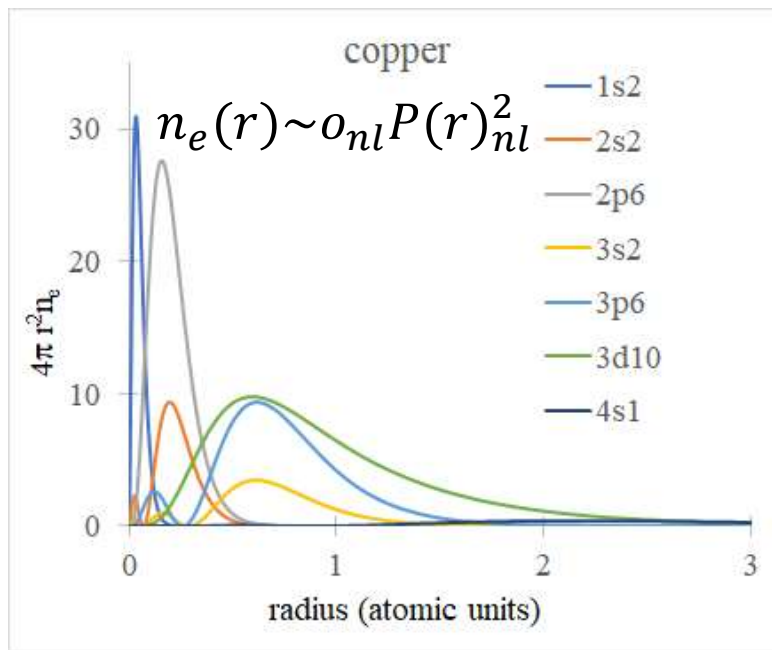
$$\int_0^{R_{WS}} 4\pi r^2 \rho dr = Z_{nuc}$$

Neutrality in the Wigner-Seitz sphere is enforced by the chemical potential  $\mu$

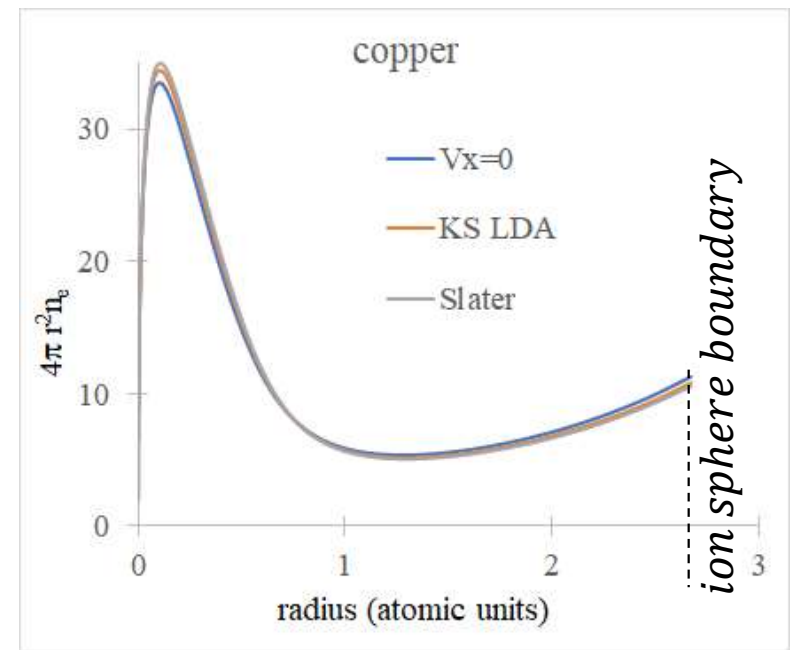
$$\nabla^2 V = -4\pi\rho$$

# The first average-atom models were the first DFT models

Through the 1930s and 1950s, development of Hartree-Fock-Slater methods in atomic physics (for isolated atomic structure calculations) led to improved exchange-correlation functionals for self-consistent field (SCF) models, and density functional theory (DFT) took off as its own field



Isolated, 0-T atomic Hartree-Fock:  
quantum, for atoms & fixed configurations



High-T,  $\rho$  Thomas-Fermi SCF AA:  
fluid adjusts to electron temperature & density

# In 1979, a fully quantum average-atom model was born

“ABANDON ALL HOPE YE WHO ENTER HERE”

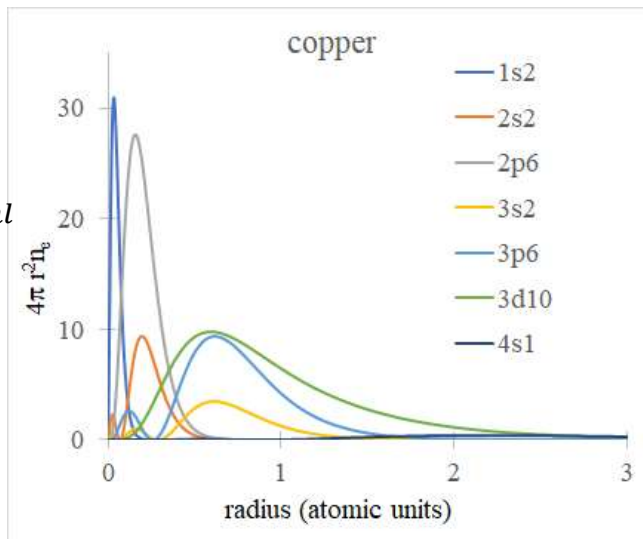
There have been many models of atoms in plasmas which have been proposed in the past fifty or sixty years. Perhaps my main advantage in undertaking the present work is that I know very little about them. This means going back to the fundamental principles and devising a model which makes the best possible use of our present day knowledge of electronic structure and of the electronic computers now available. I have called it INFERNO.

David Liberman

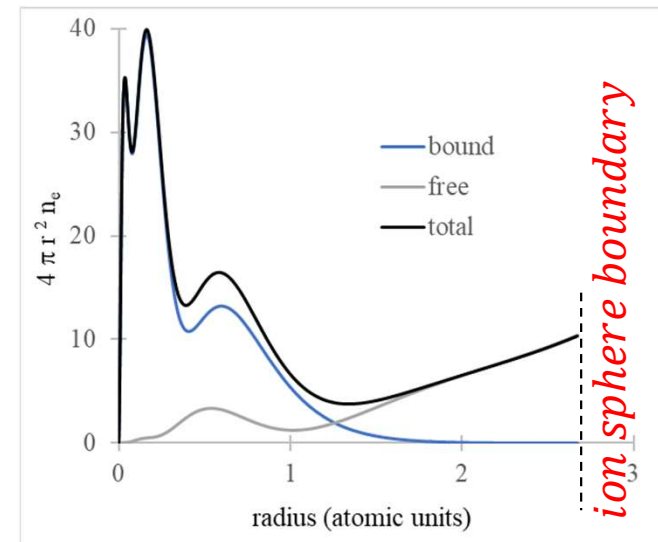
*J. Quant. Spectrosc. Radiat. Transfer* Vol. 27, No. 3, pp. 335-339, 1982

$$n_e(r) \sim \sum_{\epsilon l} \int \frac{P_{\epsilon l}^2(r)}{1 + e^{(\epsilon - \mu)/\tau}} dr$$

Isolated, 0-T  
 $n_e(r) \sim n_{nl} P(r)_{nl}^2$



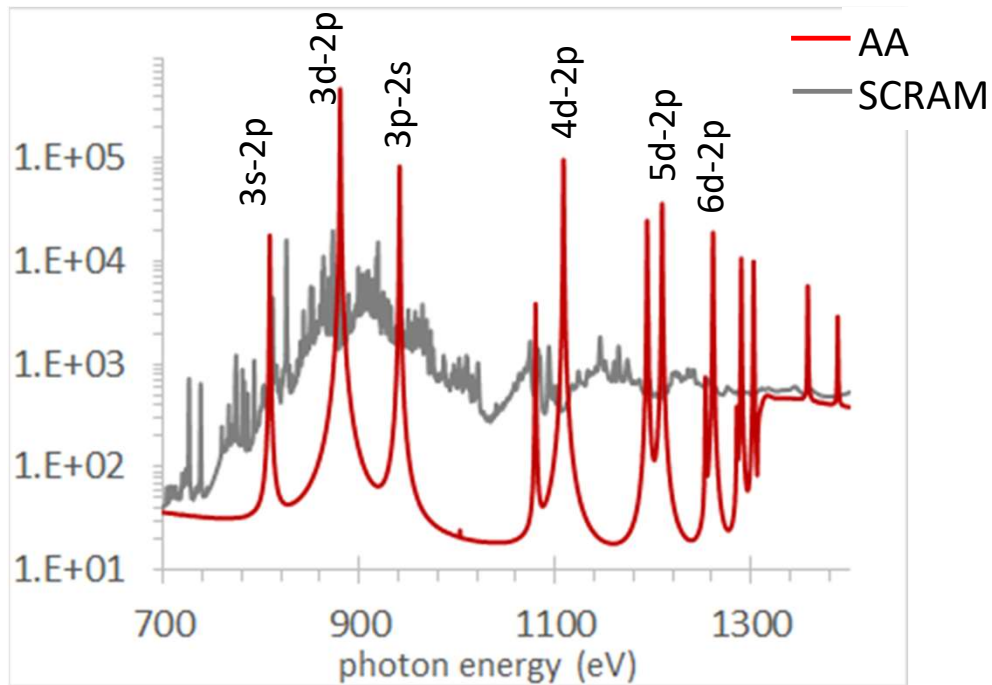
Low-T solid



Inferno *confines* the self-consistent potential in an ion sphere with Fermi-Dirac occupations for quantum electron orbitals: it natively accounts for density & degeneracy effects on atomic structure

# Average-atom models oversimplify atomic structure & spectra

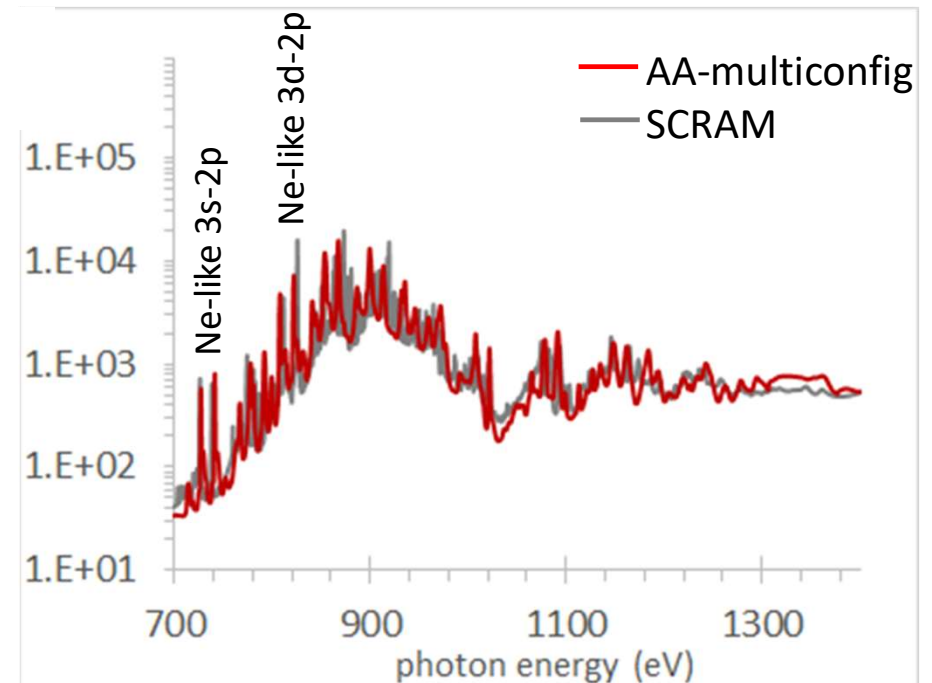
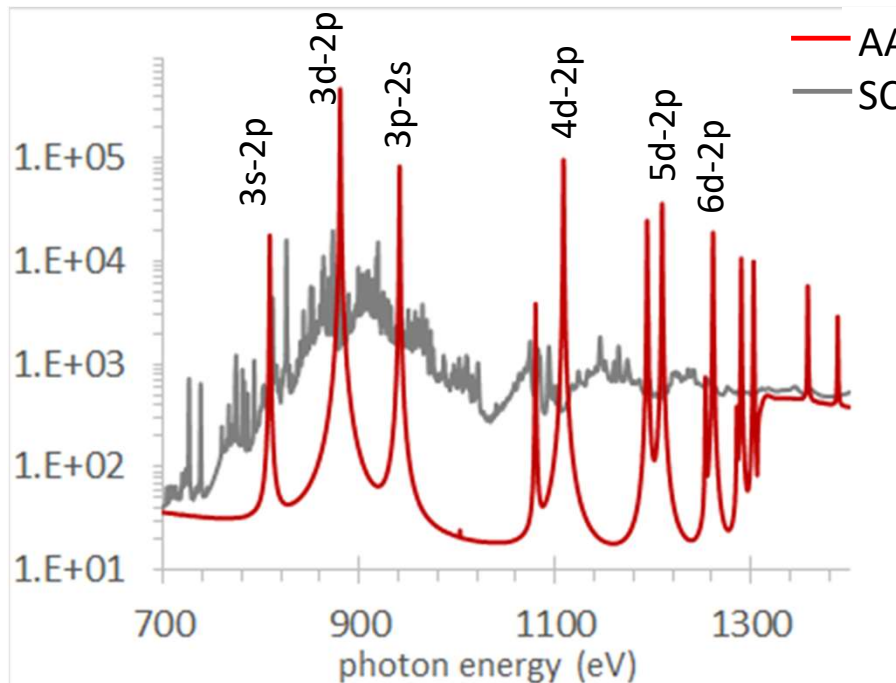
Example: L-shell iron



Average atom models have a single transition where detailed models have many

# Average-atom models oversimplify atomic structure & spectra

Example: L-shell iron

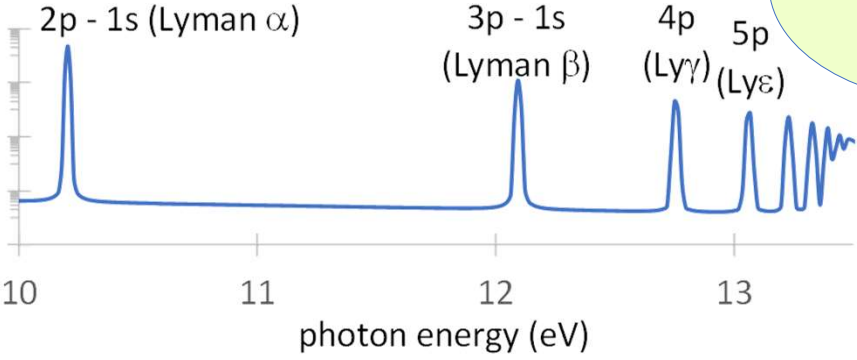
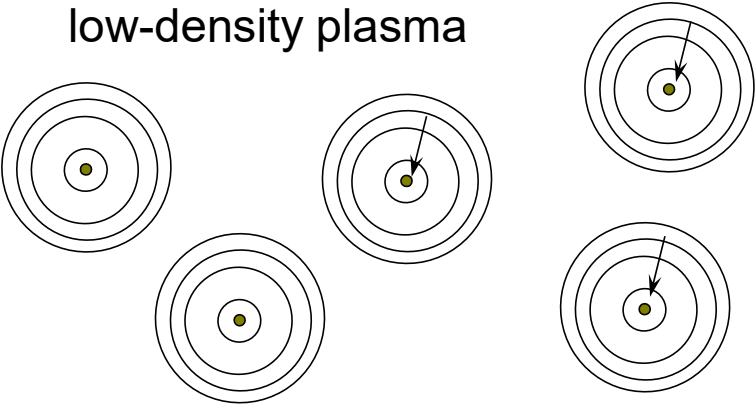


Average atom models have a single transition where detailed models have many

We can apply standard atomic physics methods to AA orbitals to refine spectra (see Rozsnyai, Hansen)

# High-density environments also modify spectroscopic signatures

low-density plasma

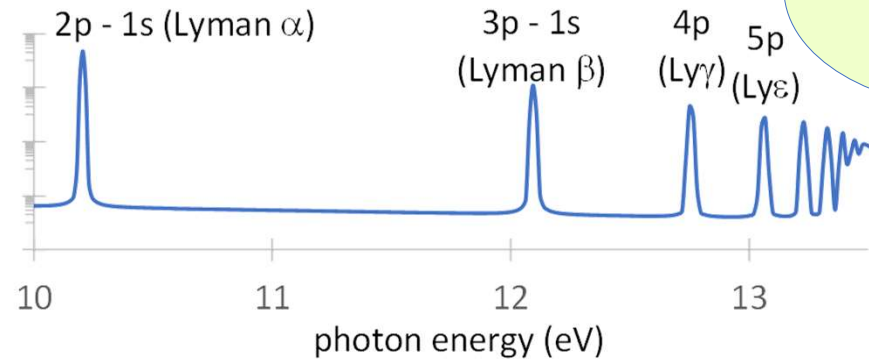
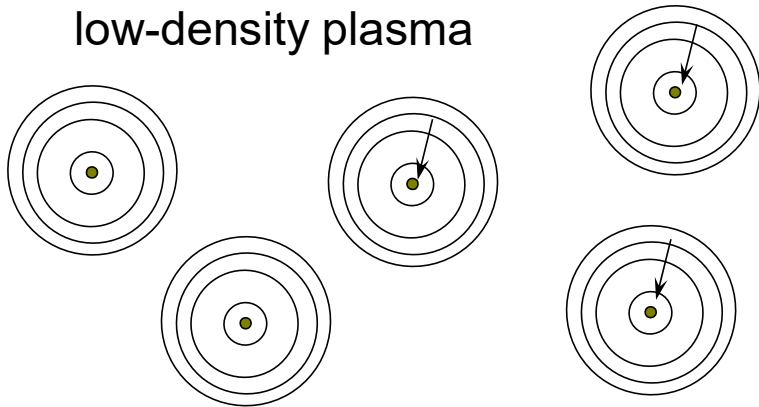


\*yawn\*



# High-density environments also modify spectroscopic signatures

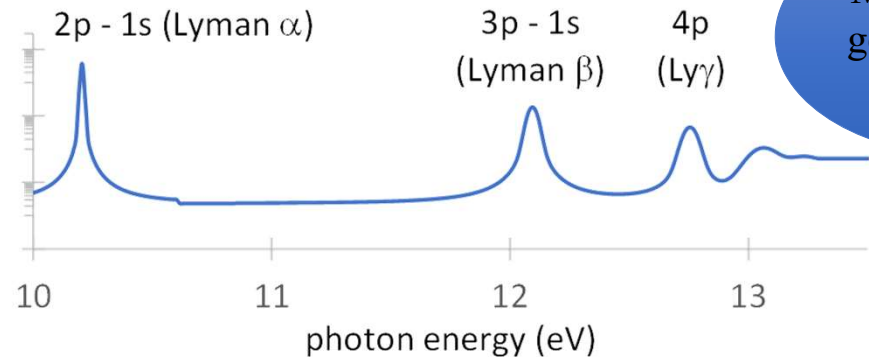
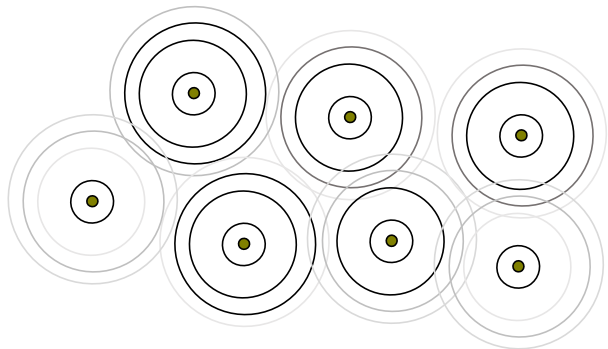
low-density plasma



\*yawn\*



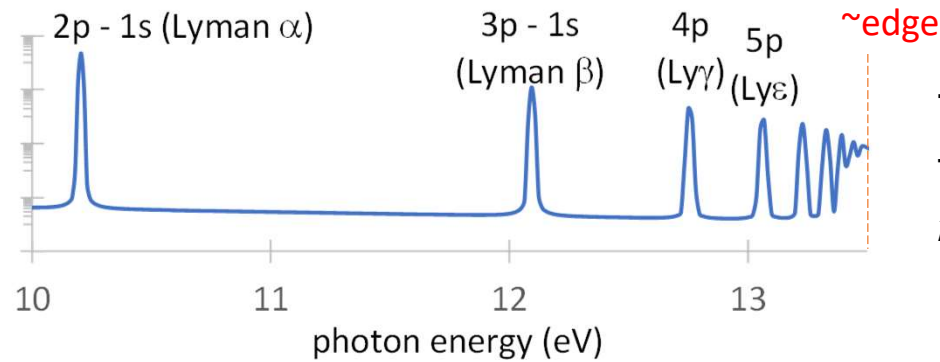
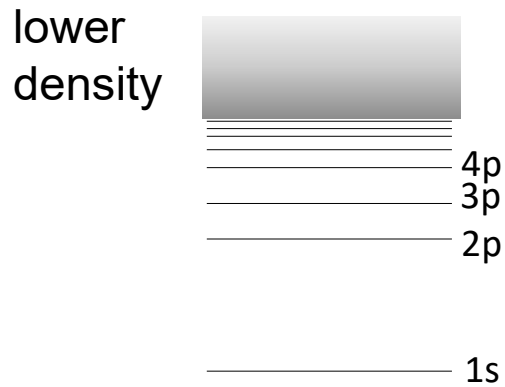
high-density plasma



My hydrogen is getting squished pretty hard!

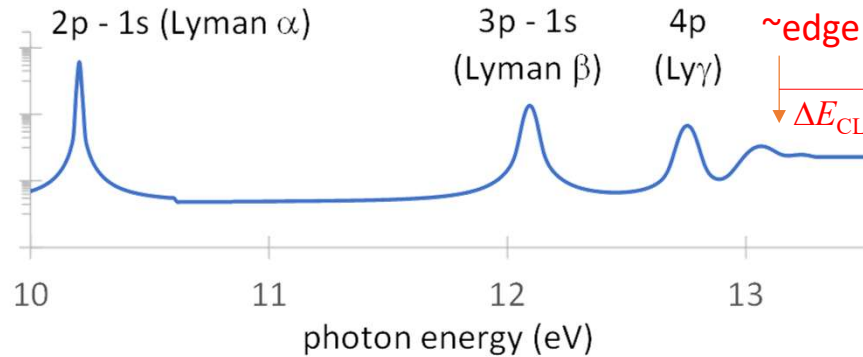
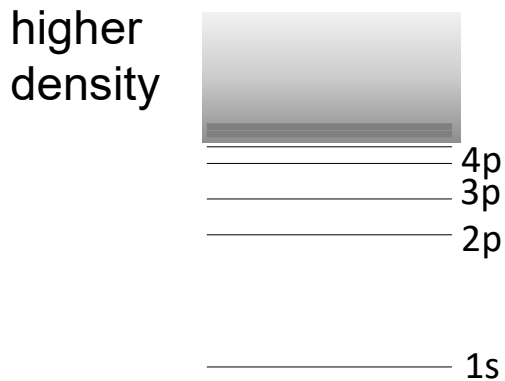


# Free-electron screening leads to continuum lowering



The Inglis-Teller limit is the highest distinct  $n$ -line:  
 $n \sim 1.7(10^{22} / n_{\text{ion}})^{0.133}(Z^*)^{0.4}$

Continuum lowering is sometimes called ionization potential depression (IPD)

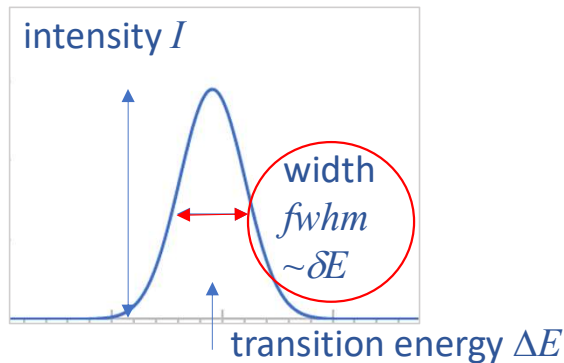


The continuum lowering energy is:  
 $\Delta E_{\text{CL}} \text{ (eV)} \sim 7.5 (Z^*+1)(n_{\text{ion}}/10^{22})^{1/3}$

Note that changes to ionization energies can significantly affect rates



# Increasing collisional rates contribute to line broadening

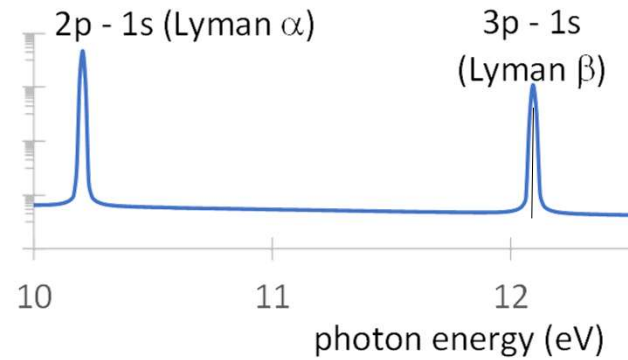
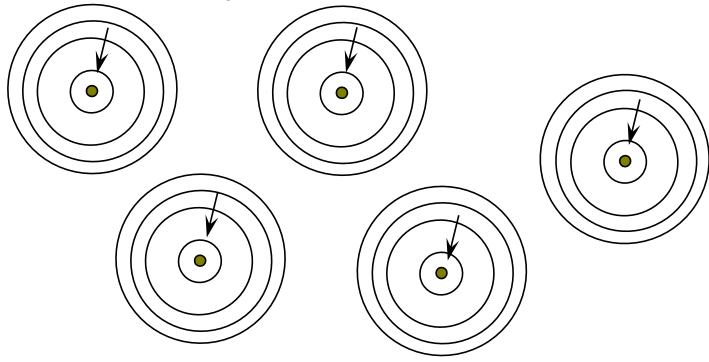


In cold low-density plasmas, lines have characteristic “natural” broadening from the uncertainty principle:  $\delta E \delta \tau = \frac{1}{2} \hbar$   
with state lifetimes  $\delta \tau = 1/A^r \rightarrow \delta E \sim \frac{1}{2} \hbar A^r$

In dense plasmas, collisional rates decrease the state lifetimes, leading to a compensatory increase in the uncertainty of the transition energy (i.e. line width)  $\delta E \sim \frac{1}{2} \hbar (A^r + C)$

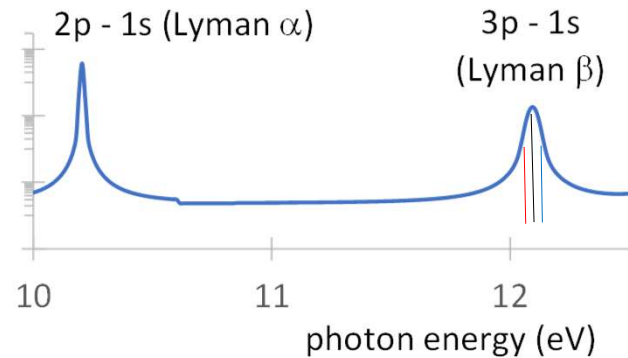
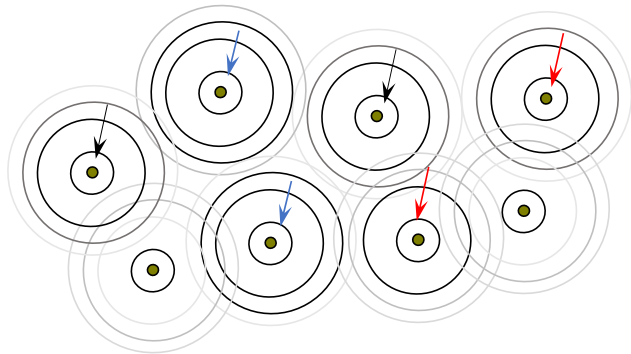
# Microfields from nearby ions also broaden lines: Stark effect

low-density plasma



Changes to local potentials lead to Stark broadening:

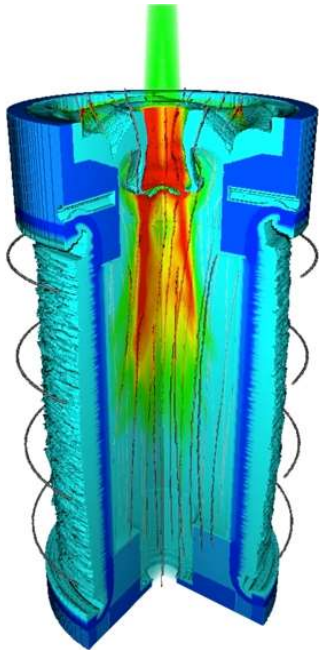
high-density plasma



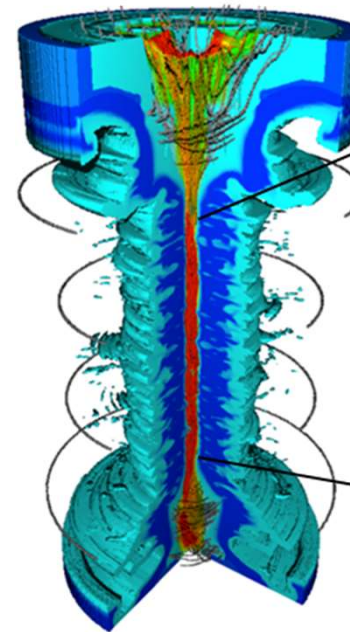
$$\text{Stark } fwhm \text{ (eV)} \\ \sim 4.3 n_{\text{up}}^2 / Z_{\text{nuc}} (n_e / 10^{22})^{0.58} \\ \text{for even } n_{\text{up}} - n_{\text{down}}$$

# Application: a fusion plasma with mix and large gradients

Magnetized liner fusion (MagLIF) is a Be liner with  $\sim 100$  ppm Fe impurities surrounding a pure-D<sub>2</sub> fuel core



The target is pre-magnetized with an axial B field and the fuel is preheated to  $\sim 100$  eV with a kJ-class laser

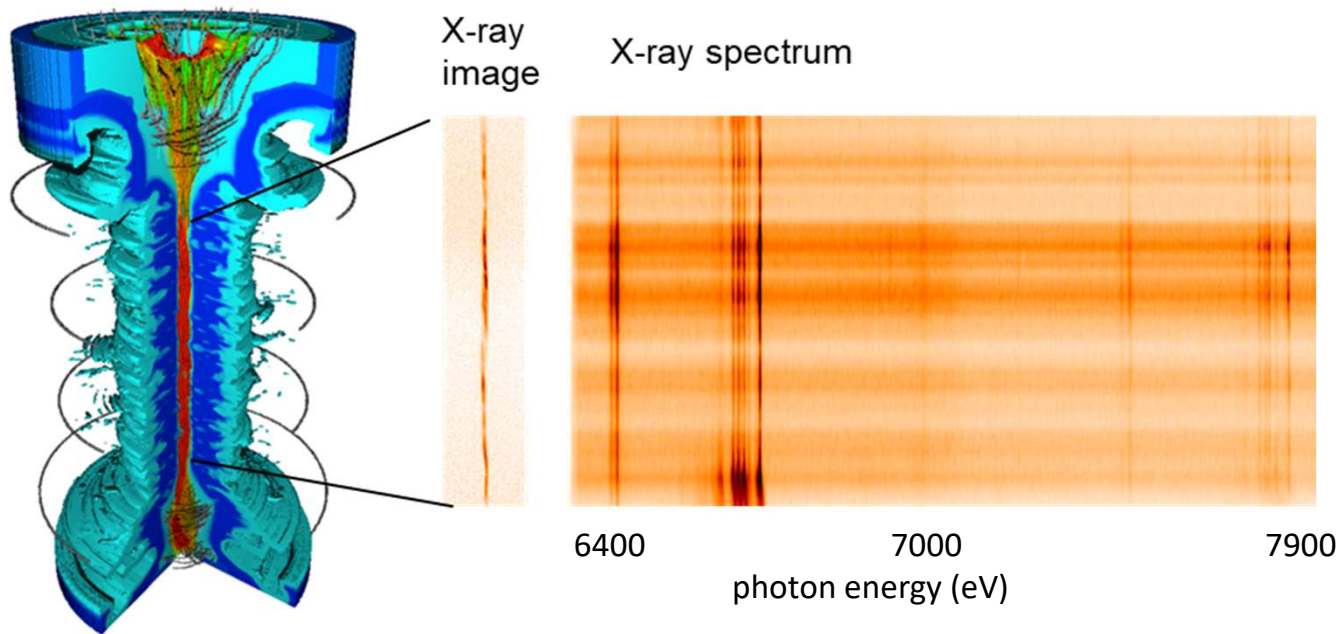


The target is imploded with the SNL Z machine's  $\sim 20$  MA of axial current, which compresses and heats the fuel to  $\sim 3$  keV temperatures

Simulation images courtesy C. Jennings

See Gomez et al, PRL 113, 155003 (2014)

# Application: a fusion plasma with mix and large gradients

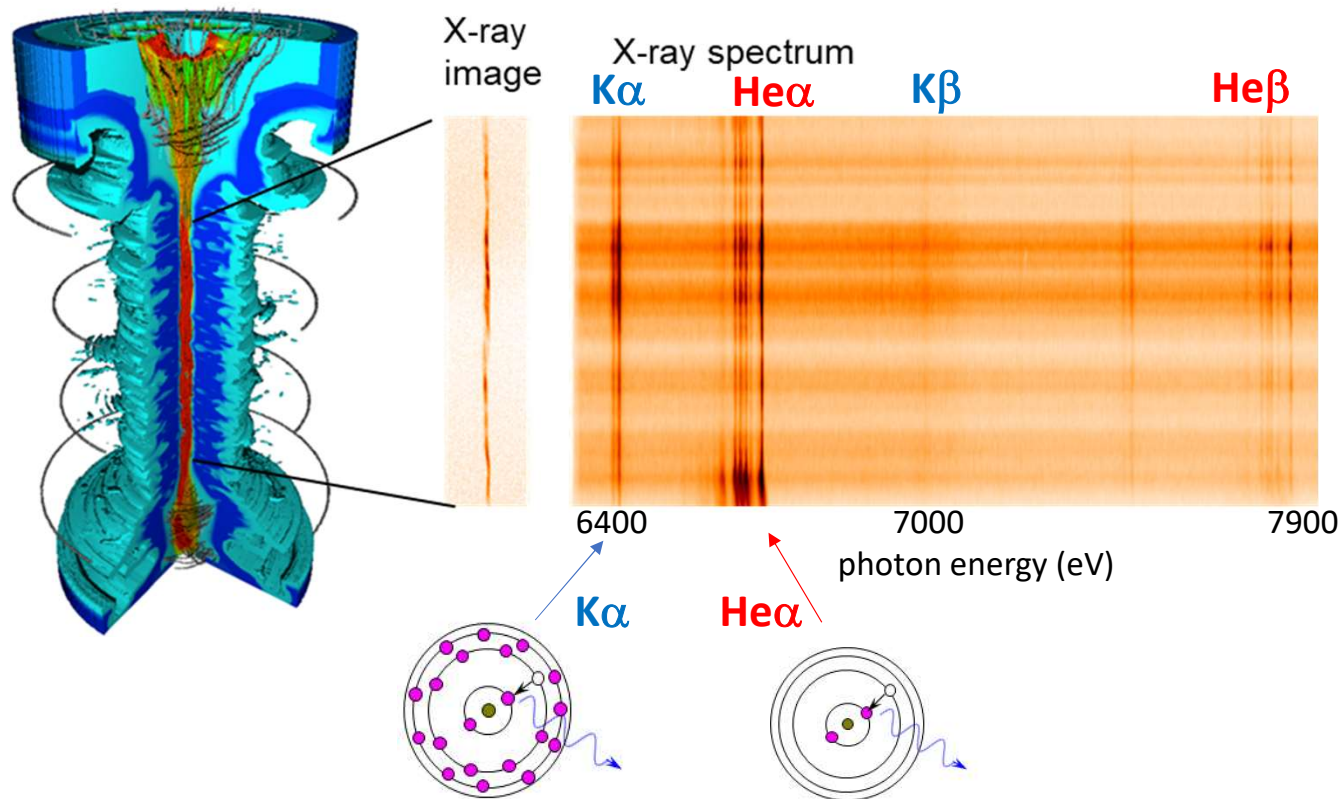


At stagnation, MagLIF targets produce fusion yields of  $\sim 1$  kJ equivalent DT neutrons and copious x-rays

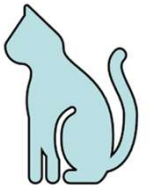
What can we learn from a high-resolution spectrum of the stagnating MagLIF plasma?

Spectrum courtesy E. Harding: absolutely calibrated 10 within 1 eV in energy, resolution  $E/\Delta E \sim 4000$  ( $< 2$  eV width)

# What can we learn from a high-resolution MagLIF spectrum?



This plasma has big gradients.

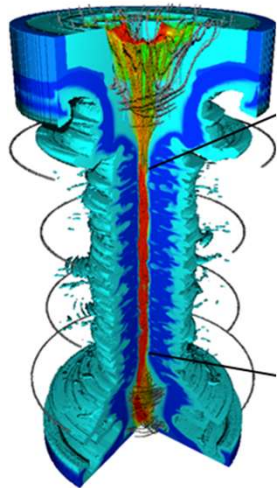
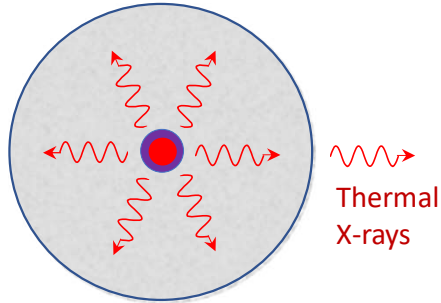


He-like iron K-shell lines:  
some of the liner, with its 100 ppm iron impurities, must reach  $\sim$  keV temperatures: mix?

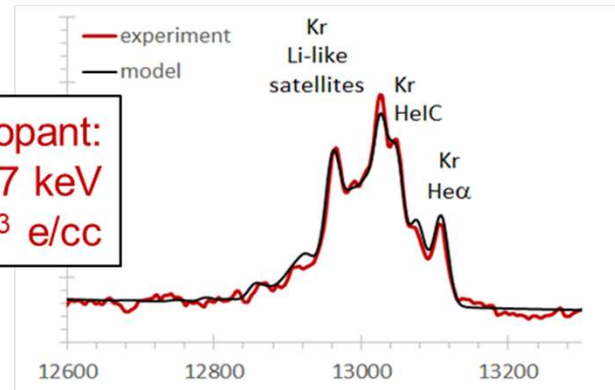
Neutral iron K-shell lines:  
Some of the liner stays cold ( $\sim$ 10 eV) and is photoionized by radiation from the hot core, producing fluorescence

# A closer look at the thermal lines gives details of gradients in the fuel

Top-down view

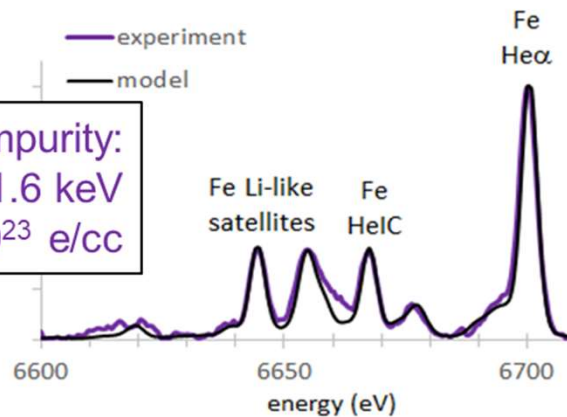


**Kr fuel dopant:**  
 $T_e^{\text{core}} = 2.7 \text{ keV}$   
 $n_e^{\text{core}} = 1 \times 10^{23} \text{ e/cc}$



Line ratios from Kr and Co co-mixed with the bulk fuel indicate core conditions

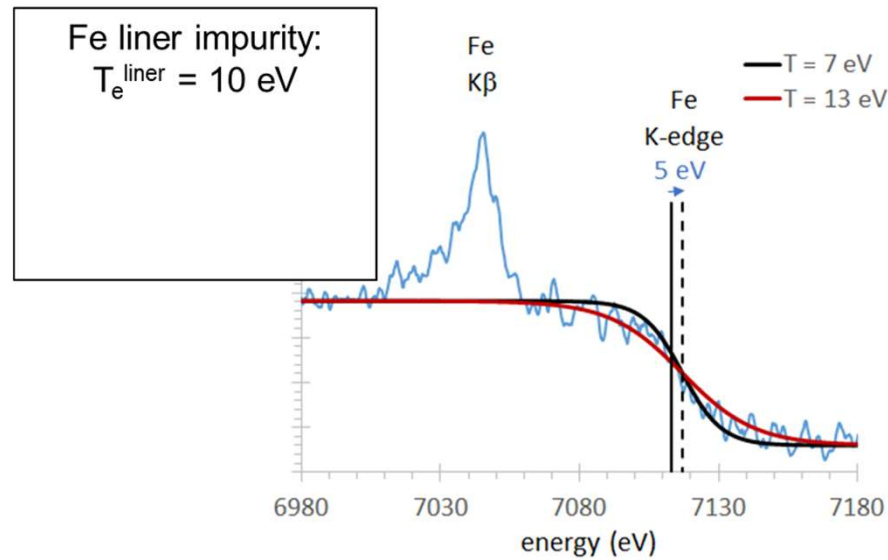
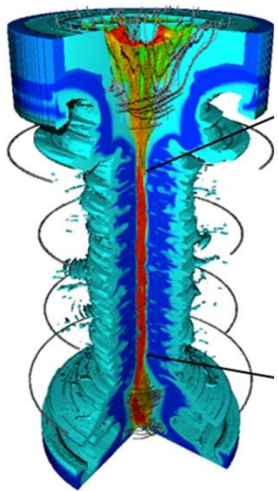
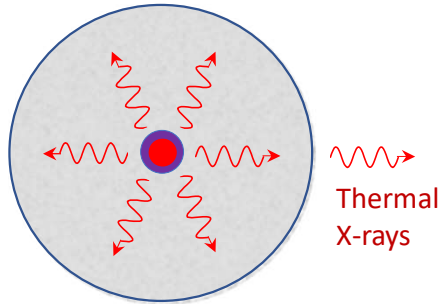
**Fe liner impurity:**  
 $T_e^{\text{mix}} = 1.6 \text{ keV}$   
 $n_e^{\text{mix}} = 2 \times 10^{23} \text{ e/cc}$



Line ratios from Fe and Ni liner impurities indicate a cooler, denser mixed layer

# A closer look at fluorescence lines & edges tells us about the liner

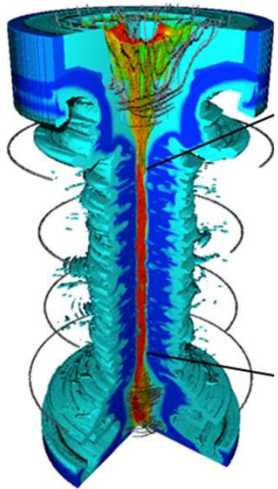
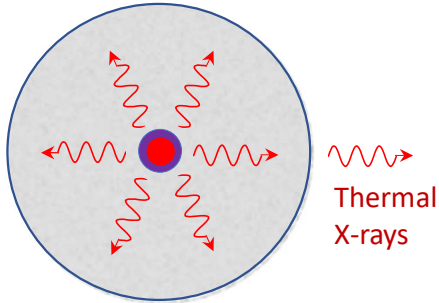
Top-down view



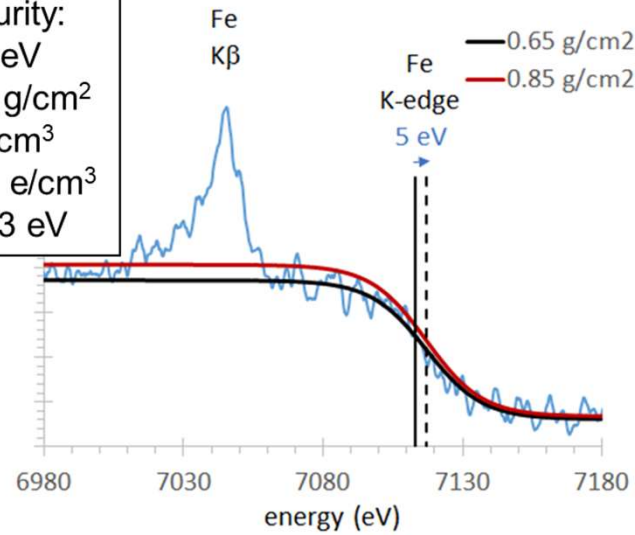
The shape of the absorption edge follows the degenerate Fermi electron distribution, indicating temperature

# A closer look at fluorescence lines & edges tells us about the liner

Top-down view



Fe liner impurity:  
 $T_e^{\text{liner}} = 10 \text{ eV}$   
 $\rho R^{\text{liner}} = 0.75 \text{ g/cm}^2$   
 $\rho^{\text{liner}} = 15 \text{ g/cm}^3$   
 $n_e^{\text{liner}} = 2 \times 10^{24} \text{ e/cm}^3$   
 $\rightarrow E_{\text{Fermi}} = 53 \text{ eV}$

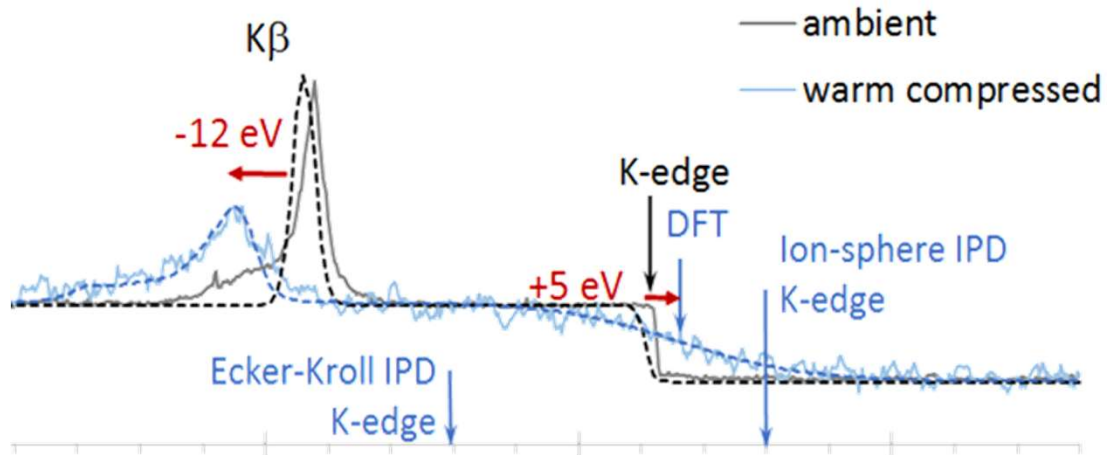


The depth of the absorption edge gives us the areal density of the liner; mass conservation and imaging constrain the density



# An intriguing red shift in $K\beta$ tells us about fundamental atomic physics

Modeled spectra (dashed) vs. measured (solid)



Looking closely at the  $K\beta$  line, we see a significant shift to lower energy in the MagLIF spectrum (blue) compared to reference data (black)

But  $K\beta$  *always only* shifts to higher energies under ionization

Roughly, ionization reduces screening of the core while compression (to 8x solid!) increases screening from excess free electrons  $\rightarrow$  leading to the red shift

This result required a high-resolution, exquisitely calibrated spectrometer and enabled us to test self-consistent atomic models and *ad-hoc* continuum lowering models

# Spectroscopy is a “Rosetta Stone\*” for the universe

---

- Spectroscopy unites the very small (quantum) with the very large (astrophysics) and very strange (extreme environments in HEDS)
- Spectroscopy tells us:
  - what elements compose a plasma
  - what conditions a plasma is in: densities and temperatures
  - can inform our understanding of atomic structure in extreme plasma environments
- Frontiers of spectroscopy include:
  - Self-consistent treatment of dense plasma effects (e.g. ICF) on atomic structure, free-electron densities of states, rates, and line shapes
  - Highly non-equilibrium systems (e.g. XFEL-pumped plasmas) where bound and free-electron occupations are non-thermal and highly transient